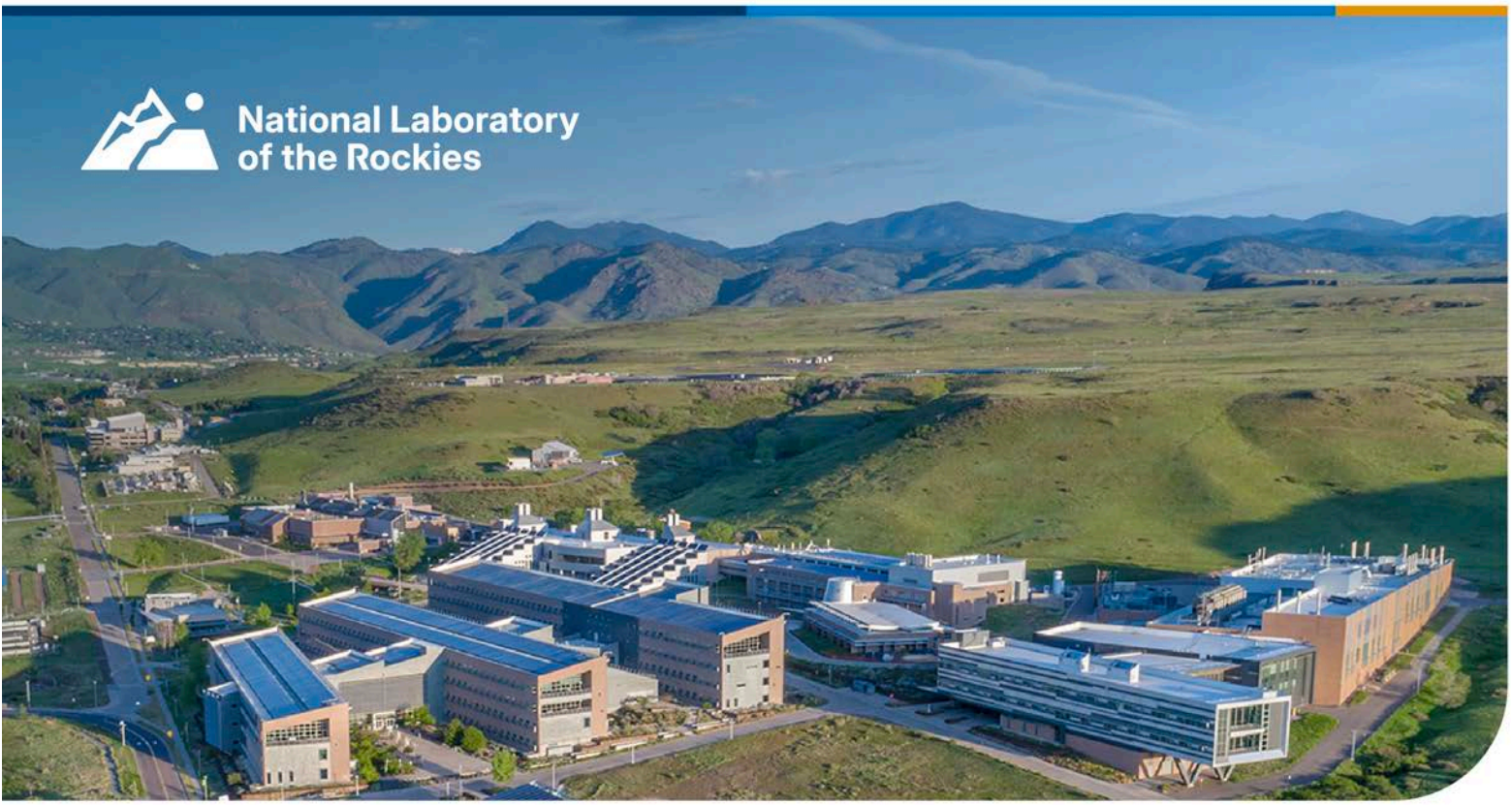

Testing and Validation of Wireless Communication Architecture for Heliostat Fields: SIPS Final Report

Matthew Muller,[1] Heyaw Getabecha,[1] and David Michael[2]

1 National Laboratory of the Rockies
2 Caribou Labs

The National Laboratory of the Rockies is a national laboratory of the U.S. Department of Energy, Office of Critical Minerals and Energy Innovation, operated under Contract No. DE-AC36-08GO28308.

This report is available at no cost from the National Laboratory of the Rockies (NLR) at www.nlr.gov/publications.

Technical Report
NLR/TP-5K00-101085
August 2026

National Laboratory of the Rockies

Testing and Validation of Wireless Communication Architecture for Heliostat Fields: SIPS Final Report

Matthew Muller,[1] Heyaw Getabecha,[1] and David Michael[2]

1 National Laboratory of the Rockies
2 Caribou Labs

Suggested Citation
Muller, Matthew, Heyaw Getabecha, and David Michael. 2026. *Testing and Validation of Wireless Communication Architecture for Heliostat Fields: SIPS Final Report*. Golden, CO: National Laboratory of the Rockies. NLR/TP-5K00-101085. https://www.nlr.gov/docs/fy26osti/101085.pdf.

The National Laboratory of the Rockies is a national laboratory of the U.S. Department of Energy, Office of Critical Minerals and Energy Innovation, operated under Contract No. DE-AC36-08GO28308.

This report is available at no cost from the National Laboratory of the Rockies (NLR) at www.nlr.gov/publications.

Technical Report
NLR/TP-5K00-101085
August 2026

National Laboratory of the Rockies
15013 Denver West Parkway
Golden, CO 80401
303-275-3000 • www.nlr.gov

NOTICE

This work was authored by the National Laboratory of the Rockies for the U.S. Department of Energy (DOE), operated under Contract No. DE-AC36-08GO28308. Funding provided by U.S. Department of Energy Office of Critical Minerals and Energy Innovation Integrated Energy Systems Office. The views expressed herein do not necessarily represent the views of the DOE or the U.S. Government.

This report is available at no cost from the National Laboratory of the Rockies (NLR) at www.nlr.gov/publications.

U.S. Department of Energy (DOE) reports produced after 1991 and a growing number of pre-1991 documents are available free via www.OSTI.gov.

Cover photo: Josh Bauer, National Laboratory of the Rockies 061725.

The National Laboratory of the Rockies prints on paper that contains recycled content.

Acronyms

BER	bit error rate
CRC	cyclic redundancy check
CST	concentrating solar thermal
dB	decibel
dBm	decibel-milliwatt
DOE	U.S. Department of Energy
DSP	digital signal processing
FOTA	firmware updates over the air
GHz	gigahertz
GMSK	Gaussian minimum shift keying
HCUCC	heliostat control unit communication controller
ISM	industrial, scientific, and medical
KB	kilobyte
kbps	kilobit per second
LBT	listen-before-talk
MAC	medium access control
MB	megabyte
Mbps	megabit per second
MHz	megahertz
NLR	National Laboratory of the Rockies
RF	radio frequency
RSSI	received signal strength indicators
SDR	software defined radio
SNR	signal-to-noise ratio
TCU	tower control unit

This report is available at no cost from the National Laboratory of the Rockies (NLR) at www.nlr.gov/publications

Executive Summary

The levelized cost of heat for concentrating solar thermal (CST) systems can be reduced by improving performance or reducing initial capital costs of heliostat fields. Caribou Labs is developing wireless controls for a CST system that improves field optical efficiency and targets heliostat costs of $\$50/m^2$. This CST system relies on a closed loop wireless control architecture. Closed loop control improves performance by dynamically adjusting heliostat aim points to maximize flux on the receiver in real time. Wireless communication to the heliostat field reduces initial capital costs by eliminating wiring and associated installation costs, a nontrivial expense for heliostat fields that may require wiring to tens of thousands of individual units. By supporting closed loop control strategies and eliminating wires, bidirectional wireless communication solutions address levelized cost of heat by simultaneously improving performance and reducing capital costs. Wireless communication remains underutilized in CST applications as a result of underdevelopment in four performance areas: reliability, throughput, scalability, and cybersecurity; all of which this project addresses. Outputs of this work include a working demonstration of a multinode communication system, clear reporting of system performance, and technical documentation of system development and architecture for reproducibility.

This report is available at no cost from the National Laboratory of the Rockies (NLR) at www.nlr.gov/publications

Table of Contents

Executive Summary ..... **iv**
1 Major Goals and Objectives **1**
2 Summary of Technical Achievements **2**
3 Impact **3**
4 Project Summary **4**
4.1 Hardware 4
4.1.1 System Description and Basic Architecture 7
4.1.2 Detailed Medium Access Control Layer Message Structure and Spectral Frequency Allocation 8
4.1.3 Design for Heliostat Field Size and Communication Rate 11
4.1.4 Other Features of Wireless Architecture 12
4.1.5 Cost Breakdown 15
4.1.6 Flatirons Field Test Layout 15
4.2 Simulation of the Flatirons Field 19
4.2.1 Simulation Results 21
4.3 Benchtop Testing and Initial Field Installation and Troubleshooting 24
4.3.1 Data Collection and Results 27
4.4 Key Field Test Outcomes 31
4.5 Lessons Learned 31
4.5.1 System Power Supply and Consumption 31
4.5.2 Manufacturing Concerns 32
4.5.3 Hardware-Level Lessons 32
4.5.4 Software-Level Lessons 33
5 Next Steps **35**
APPENDIX **37**

This report is available at no cost from the National Laboratory of the Rockies (NLR) at www.nlr.gov/publications

List of Figures

Figure 1. Detailed hardware inclusions on the open-source HCUCC board 4
Figure 2. The secondary board that plugs directly into the HCUCC for providing battery and solar power 5
Figure 3. Physical realization of the HCUCC hardware, including a small solar cell for providing power and the outdoor enclosure used for testing at the Flatirons field 5
Figure 4. Desktop testing of the HCUCC. 6
Figure 5. The TCU hardware includes a Raspberry Pi, which is below the heat sink in the upper center of the picture. 6
Figure 6. The tower control hardware mounted in an outdoor enclosure for mounting on the Flatirons met tower. 7
Figure 7. A graphic of the asymmetric communication between the TCU and tens of thousands of heliostats through controlled frequency allocation 8
Figure 8. Communication between the TCU and heliostats, in which multiple heliostats are packed into jumbo frames that go out from the TCU 9
Figure 9. The message structure for an uplink jumbo frame. 10
Figure 10. The message structure for the downlink message from 1 HCUCC to the TCU (an individual responds to a delivered message from the tower) 10
Figure 11. An example of the spectrally dependent uplink and downlink channels for the 915-MHz ISM band. 11
Figure 12. An example of periodic beacons being sent over an uplink channel to provide for network node acquisition 13
Figure 13. Comparison of CLER, an open-source DSP library for the SDR, versus existing software that was not going to work for the SDR at the Flatirons 14
Figure 14. The upper image shows a signal sent with GMSK (time verse frequency), and the lower image shows a breakdown of extraction of message parts. 15
Figure 15. Satellite map of the Flatirons campus with overlay of 100 HCUCC nodes. 16
Figure 16. Mounting of the TCU enclosure and transmitting and receiving antennas on the met tower to the west of node 21 17
Figure 17. TCU is mounted ~30 meters high 18
Figure 18. One of the HCUCCs mounted in their outdoor enclosures at approximately 1.3 meters high 19
Figure 19. Block diagram for radiofrequency channel emulation 20
Figure 20. The organization of a simulation run 21
Figure 21. MAC layer encryption as incorporated with radiofrequency emulation 21
Figure 22. Results for coding and decoding uplink messages considering different parity bits 22
Figure 23. Results for coding and decoding downlink messages considering different parity bits 23
Figure 24. The simulated package error rate for different burst lengths and redundancy levels 24
Figure 25. Spectral data in the 915-MHz band collected using the tower SDR shows that there are large amounts of interference from other ongoing communication at the Flatirons. 26
Figure 26. An additional example of spectral data in the 915-MHz band collected by the tower SDR highlights communication per FSK, LoRa, PSK/QPSK (none of which come from HCUCCs) 27
Figure 27. The figure shows the heliostats in dark blue that were active during the data collection on 2/26/26 28
Figure 28. Median HCUCC Rx power in dBm 29
Figure 29. Relative calculated SNR in dB (power at the TCU Rx antenna minus the noise floor) 29
Figure 30. HCUCC message drop rate 30
Figure 31. (left) Steps to improving/fixing the existing 100-node test bed. (right) Steps to developing an off-the-shelf system for the heliostat fields. 36

List of Tables

Table 1. Key Results From Both the 100-Node Simulation and 74 Nodes in the Field 30
Table A-1. Parts List and Associated Pricing for Printing 30,000 HCUCC Boards 37

This report is available at no cost from the National Laboratory of the Rockies (NLR) at www.nlr.gov/publications

1 Major Goals and Objectives

The objective of this project is to demonstrate a wireless architecture and hardware at the National Laboratory of the Rockies (NLR) Flatirons campus that is valuable to the entire heliostat industry. Note that the Flatirons is an outdoor test space with photovoltaic systems and other existing equipment, but it is not a heliostat field. The field test is intended to demonstrate performance that will work for any heliostat (latency of approximately hundreds of milliseconds), reliability at distances between 10 and 1,500 m, versatility to various heliostat controls and design needs, and costs in line with U.S. Department of Energy (DOE) heliostat targets of $\$50/m^2$. Additionally, the hardware will be made open source for easy adoption by others in the concentrating solar thermal (CST) industry.

This report is available at no cost from the National Laboratory of the Rockies (NLR) at www.nlr.gov/publications

2 Summary of Technical Achievements

Hardware was engineered, manufactured, and delivered to NLR for a 100-node network at the Flatirons campus. The 100-node network was both simulated and tested in the field. Through this process, the following were achieved:

- An open-source repository for manufacturing low-cost (~$30/heliostat) components for wireless communications
- Full documentation of the architecture, communication layers, and messaging structure
- Software for both the software defined radio (SDR) and heliostat control unit communication controller (HCUCC)
- Simulation software for the Flatirons system
- Inclusion of protocols/encryption for making the network cyber secure
- Introduction of a lightweight, open-source framework for programming SDRs: CLER which can be found at *https://cariboulabs.github.io/cler/*.
- Validation of the hardware and performance through data collection at Flatirons
- De-risking of the architecture and hardware for sub-second communication and scale-up to tens of thousands of heliostats. (Although thousands of heliostats were not tested, the data collected demonstrate the design is sound and there are sufficient frequency bands for achieving control of tens of thousands of units.)
- An understanding of the remaining or future work to be off-the-shelf ready.

This report is available at no cost from the National Laboratory of the Rockies (NLR) at www.nlr.gov/publications

3 Impact

The project delivered and validated wireless communication hardware that can be scaled to fields of tens of thousands of heliostats. The hardware is currently open source and can be manufactured at volume to achieve the cost of less than $30 per heliostat. Although there are further costs and development time needed to be off-the-shelf ready, the field validation demonstrated round-trip tower communication latency of 21 ms under heavy interference at the Flatirons field. The Flatiron HCUCC field test measured 74 heliostat units at ~910 megahertz (MHz) with a Gaussian minimum shift keying (GMSK) wireless control network. GMSK provides exceptional spectral efficiency, extended battery life, and high resilience to noise (similar techniques are used in Bluetooth and other wireless networks). The maximum heliostat-to-tower range was ~900 m, while signal strength was sufficiently strong to assume 1.5-km transmission distances are within range for the architecture. There are currently no off-the-shelf ready wireless communications systems that have been optimized to support the DOE cost target of $\$50/m^2$ for heliostats.

This work is distinct from other DOE/HelioCon-funded heliostat wireless projects with Arizona State University and Solar Dynamics in its communication rate of 1 Hz or greater, optimization specific for heliostat fields, cost per heliostat, or its technology readiness level. For more details, a 2026 HelioCon report is being published to provide a clear comparison of these three unique projects. The approach in this work is estimated to need an additional $600,00 to $800,000 and a 1-year well-defined project to become a commercially available, secure, and reliable architecture for heliostat fields.

This report is available at no cost from the National Laboratory of the Rockies (NLR) at www.nlr.gov/publications

4 Project Summary

4.1 Hardware

Figure 1 and Figure 2 provide details of the open-source HCUCC board and solar charging control that are tested in this project. One hundred boards were delivered to NLR for benchtop testing and then eventual field deployment. The HCUCC was intentionally designed with low-cost components that allow manufacturing at volume for approximately $30 per board. Figure 3 through Figure 6 provide the physical realizations and descriptions of the HCUCC hardware and tower control unit (TCU) shipped to NLR for benchtop testing and for installation of the 100-node network at the Flatirons campus.

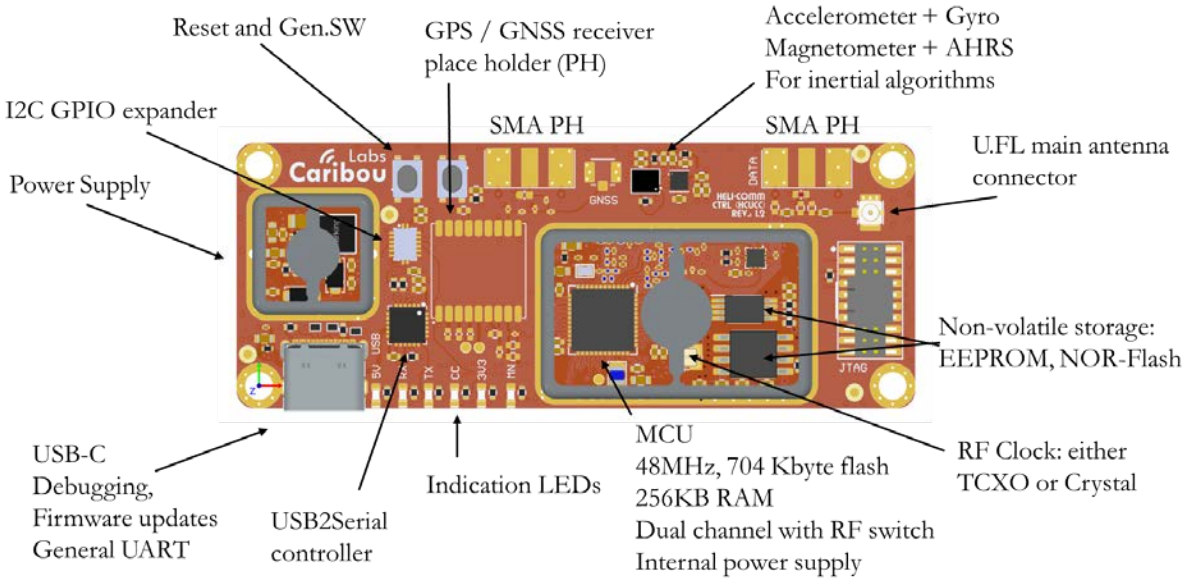

Figure 1. Detailed hardware inclusions on the open-source HCUCC board

This report is available at no cost from the National Laboratory of the Rockies (NLR) at www.nlr.gov/publications

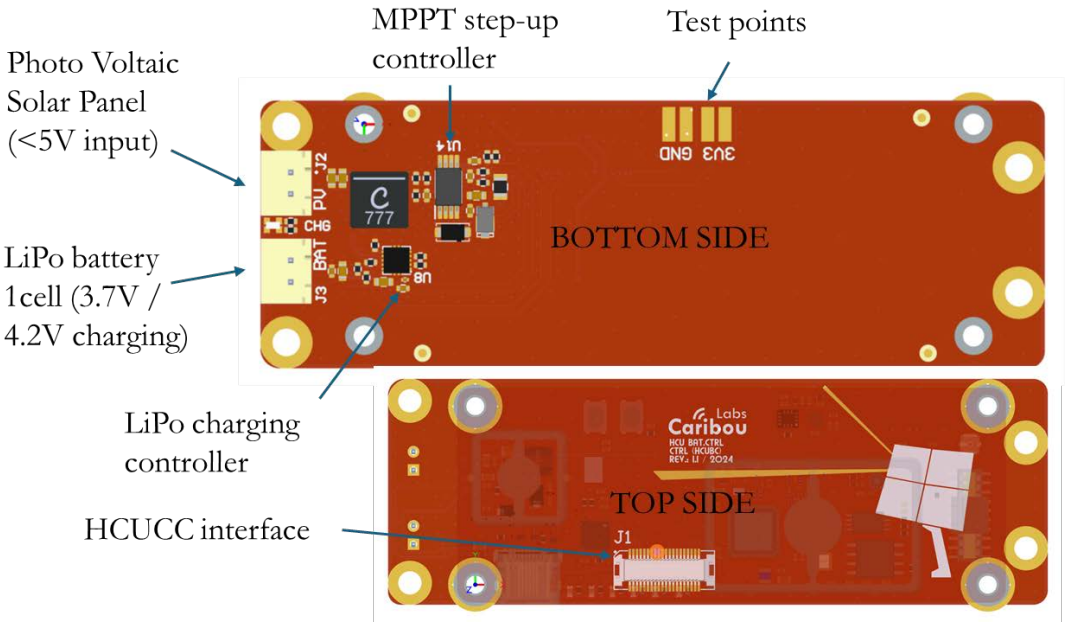

Figure 2. The secondary board that plugs directly into the HCUCC for providing battery and solar power

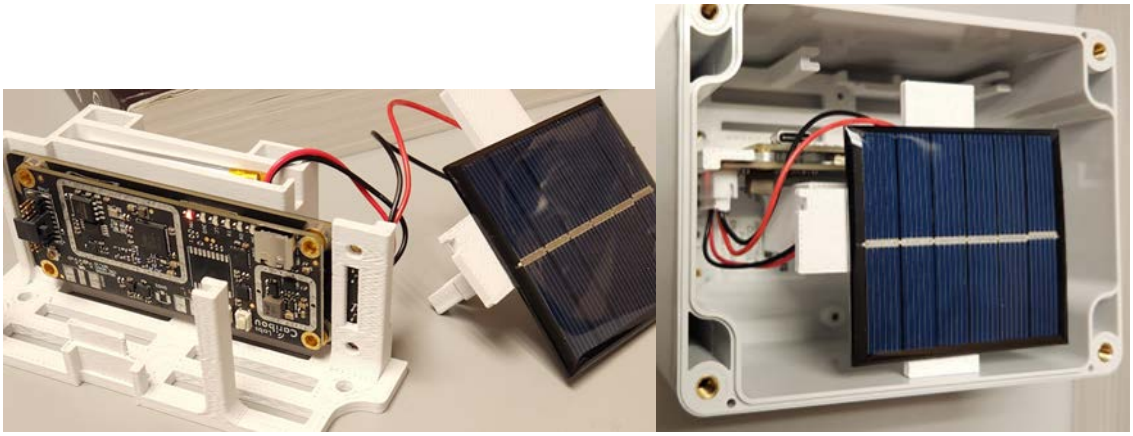

Figure 3. Physical realization of the HCUCC hardware, including a small solar cell for providing power and the outdoor enclosure used for testing at the Flatirons field

This report is available at no cost from the National Laboratory of the Rockies (NLR) at www.nlr.gov/publications

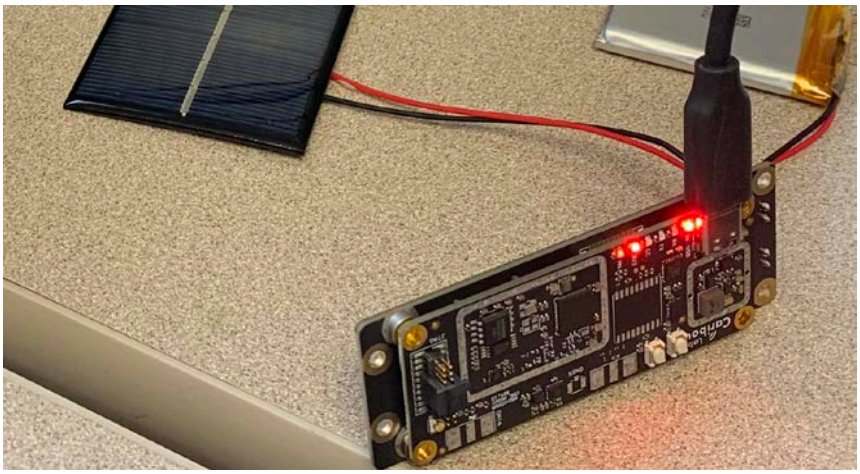

Figure 4. Desktop testing of the HCUCC.

The unit is plugged into a laptop for firmware updates and verification of communication. Red LEDs indicate the unit is both transmitting and receiving messages.

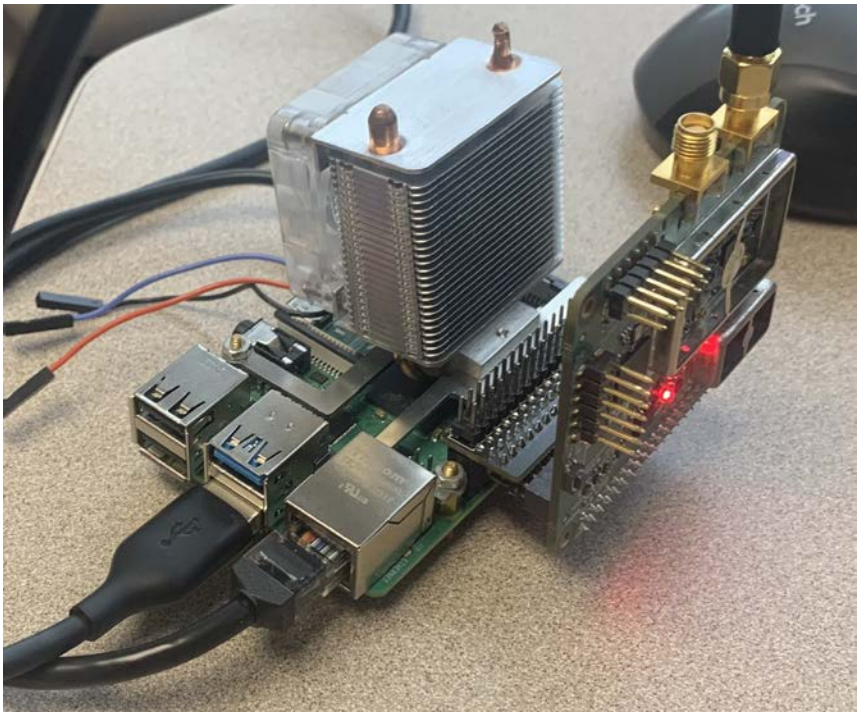

Figure 5. The TCU hardware includes a Raspberry Pi, which is below the heat sink in the upper center of the picture.

To the right (plugged in to the Raspberry Pi) is a Caribou Labs SDR for transmitting jumbo frames to the heliostat field. At the top right, the SDR connector provides direct link to the receiving antenna and handles parallel incoming messages from fielded HCUCCs. In the lower left the USB connector leads to an HCUCC, which is connected to the transmitting antenna. Power is provided over the ethernet connector in the lower left. The Caribou Labs SDR (~$100) in use here is sufficient for the field test of 100 units, whereas in a field of tens of thousands of heliostats, an SDR accommodating the full-frequency bandwidth at 915 MHz or 2.5 gigahertz (GHz) would cost approximately $2,000.

This report is available at no cost from the National Laboratory of the Rockies (NLR) at www.nlr.gov/publications

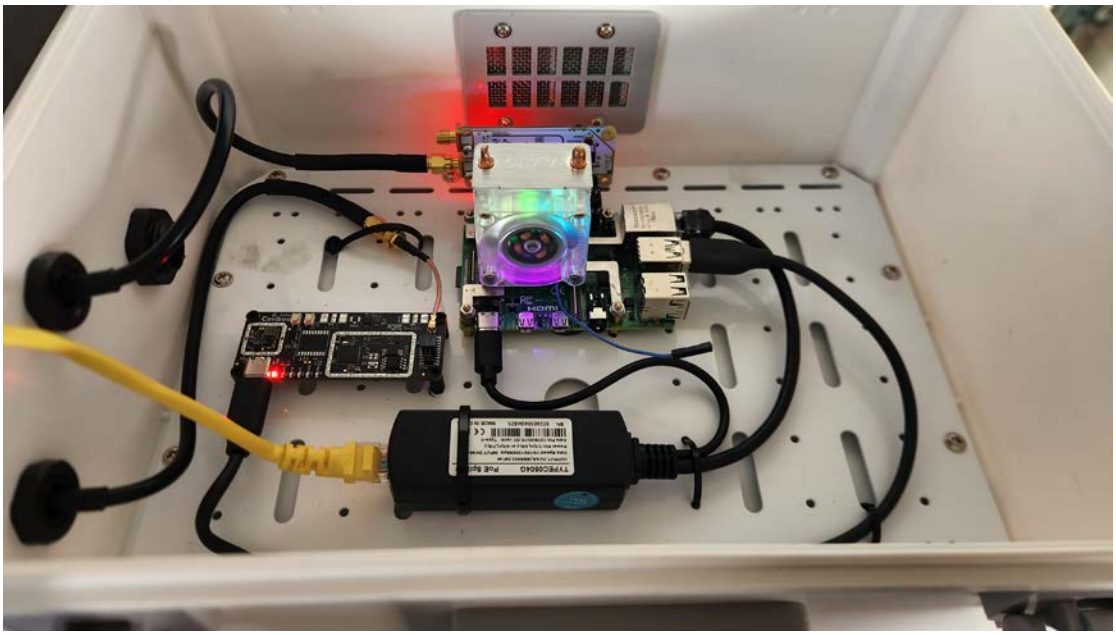

Figure 6. The tower control hardware mounted in an outdoor enclosure for mounting on the Flatirons meteorological tower.

The HCUCC can be seen on the left, the Raspberry Pi and SDR in the upper center portion and the power over ethernet box in the lower center. An ethernet cable and two antenna cables exit through the side of the enclosure.

4.1.1 System Description and Basic Architecture

The wireless communication hardware associated with this work generally is designed to be operated as follows:

- Radio communication at 915 MHz and 2.4 GHz (software controlled)
- Communication link properties:
    - Telemetry/control refresh rates can be greater than 5 Hz but are dependent on field size and communication frequencies chosen.
    - Point-to-point communication exists between tower and heliostats (no hopping).
    - TCU computer fully controls frequency allocation for transmitting and receiving and synchronizes the system.
    - All fielded HCUCCs implement listen-before-talk protocol.
    - Intended maximum communication range is approximately 1.5 km.
    - Firmware updates over the air (FOTA) capabilities are planned, but additional funds are needed to write and vet robust software (the system must default to a stable firmware version in the event of any errors occurring during a software update).
    - Modulation: GMSK, signal-to-noise ratio (SNR)> 5 decibels (dB), bandwidth-time product = 0.3, modulation Index = 0.5 (these specifications for GMSK result in high spectral efficiency)

This report is available at no cost from the National Laboratory of the Rockies (NLR) at www.nlr.gov/publications

    - Cybersecurity (encryption and authentication), AES-256-CTR mode cipher
- Open-source hardware at github.com/cariboulabs/heliostat_controller.git.

An asymmetric communication approach is employed in which the TCU transmits jumbo frames that contain messages for multiple HCUCCs while each HCUCC responds separately. Additionally, the TCU transmits higher power than the HCUCCs. The TCU includes a Linux computer (Raspberry Pi) for computations, an SDR for receiving messages (a CaribouLite for the field validation, where a USRP B206 mini is planned for tens of thousands of heliostats and can handle both transmitting and receiving messages), and an HCUCC transmitting messages to the HCUCCs or heliostats in the field. The combination of the CaribouLite SDR and HCUCC allow simultaneous receiving and transmitting of messages. Power is provided to the TCU from the grid over ethernet, where transmitting power is greater than 34 decibel-milliwatts (dBm) and 1 megabits per second (Mbps) (considered the uplink side of the system). HCUCCs are mounted on each heliostat and can send messages to the TCU at ~19 dBm and 100 kilobits per second (kbps) (considered downlink side) and are powered by a small battery and solar panel. The HCUCC can be attached to a heliostat controller or serve as the controller if additional motor or actuator drivers are incorporated. The HCUCC was specifically designed to hit low-cost targets per heliostat and to use low-power to avoid heliostat field trenching. Figure 7 provides a graphic of the asymmetric communication between a TCU and many HCUCCs.

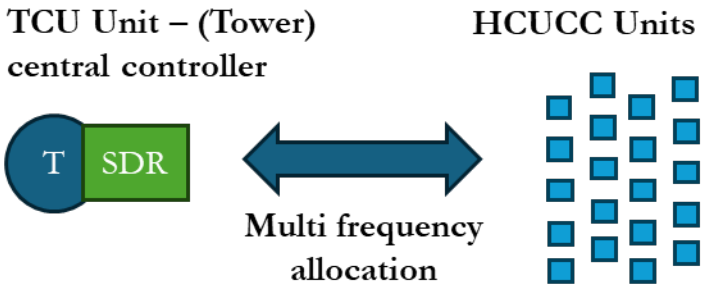

Figure 7. A graphic of the asymmetric communication between the TCU and tens of thousands of heliostats through controlled frequency allocation

4.1.2 Detailed Medium Access Control Layer Message Structure and Spectral Frequency Allocation

The TCU transmits uplink jumbo frames, where a single jumbo frame contains messages for 14–18 HCUCCs (16 in the Flatirons testing). The header within the jumbo frame identifies which heliostats the message belongs to, and when the match occurs, each HCUCC returns a short response with status on its sequential order within the jumbo frame. In the meantime, the TCU continues to simultaneously transmit and receive messages. Figure 8 provides a schematic of communication between the TCU and heliostats, in which multiple heliostats are packed into jumbo frames that go out from the TCU. The TCU loops through transmitting to all N jumbo frames, in which a 5-Hz update is planned, but communication rate is software controlled and can be adapted as needed for field size. Because the TCU has antennas for parallel transmitting and receiving, each heliostat or HCUCC response can be received while still looping through transmitting of jumbo frames.

This report is available at no cost from the National Laboratory of the Rockies (NLR) at www.nlr.gov/publications

Figure 8. Communication between the TCU and heliostats, in which multiple heliostats are packed into jumbo frames that go out from the TCU

An example jumbo frame message structure is shown in Figure 9. The jumbo frames contain optionally encrypted messages using AES-256-CTR mode cipher. This is a symmetric encryption method using a 256-bit key to turn a block cipher into a stream cipher and is highly efficient for rapid communication. Within the header, multiple HCUCC IDs are addressed, all at once. Forward error correction, mitigating both random and burst noise, is used to correct errors and reconstruct corrupted data, reducing packet error rate. Cyclic redundancy checks (CRC) provide header and payload validation, to maintain the industry standard 6-bit Hamming distance error detection assurance. In this example, the payload data contain communal data for all heliostats (e.g., weather, sun position) and unit-specific control data (e.g., adjustments to azimuth and elevation tracking). The downlink messages, transmitted by the heliostats (see Figure 10), contain a similar message header, while the payload is smaller, containing a single heliostat information. The opcode defines what is in the message structure and up to 256 opcodes can be easily defined per C++ or Python code as needed for different heliostat fields.

This report is available at no cost from the National Laboratory of the Rockies (NLR) at www.nlr.gov/publications

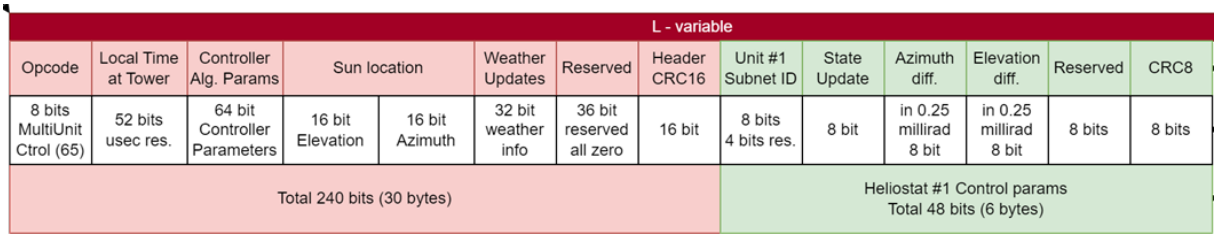

Figure 9. The message structure for an uplink jumbo frame.

Only 1 of 16 HCUCC/heliostats is shown here for simplicity.

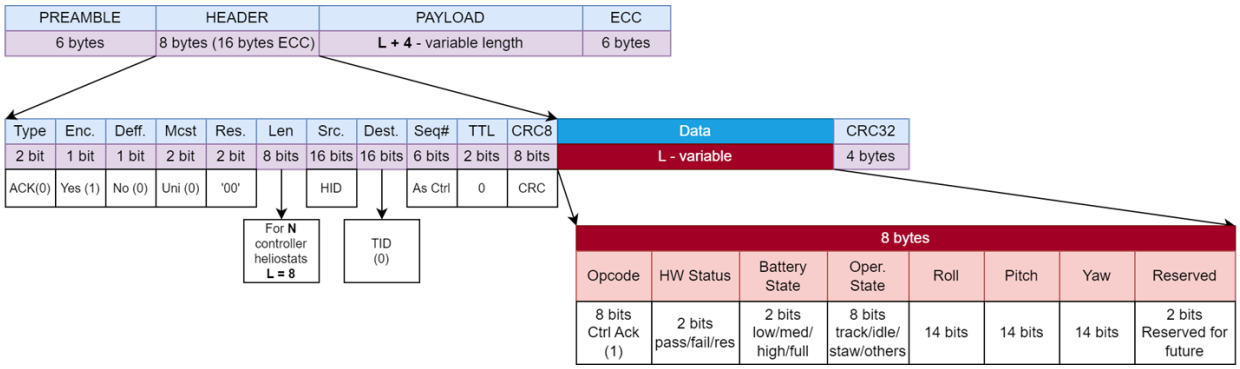

Figure 10. The message structure for the downlink message from 1 HCUCC to the TCU (an individual responds to a delivered message from the tower)

In general, the medium access control (MAC) layer in radio communication is responsible for managing spectrum, setting transmission times, handling data framing, and managing retransmissions. The MAC layer network channels are divided into spectrally dependent uplink and downlink bands, with an example of this shown in Figure 11. In Flatirons testing, the 915-MHz industrial, scientific, and medical (ISM) band (26 MHz of width) was implemented with the assumption it would not be congested for small-scale testing. The band can be further expanded to the 2.4-GHz ISM band, which provides a larger bandwidth of 83.5 MHz. Figure 11 shows an example subdivision into 7 channels (frequency sub-bands) with 14 heliostats each, while field implementation at the Flatirons includes 16 HCUCCs per band. Considering the uplink operates at 1 Mbps with GMSK and with guarding between channels, 1.5 MHz of bandwidth was allocated or designed for a single jumbo frame channel, where 7 such channels occupy 10.5 MHz of bandwidth. On the downlink side, a single HCUCC or heliostat operates at 100 kbps. A 130-kHz bandwidth is allocated/designed for a single heliostat, taking into account GMSK and guarding. Considering 16 heliostats per channel, this equates to 2.08 MHz allocation per downlink channel and 14.6 MHz for seven downlink channels. The TCU computer controls spectral allocation in each message sent to a HCUCC (i.e., the message from the TCU specifies at what frequency the individual HCUCC should respond). Frequency allocation is not static but rather varied by the TCU to optimize performance and respond to congestion or potentially jamming (note that, in the Flatirons testing, the TCU randomized rather than optimized frequency assignments).

The MAC layer also includes radio traffic control through listen-before-talk (LBT) protocols. LBT implies that HCUCC radio must listen on its intended frequency to determine that channel

This report is available at no cost from the National Laboratory of the Rockies (NLR) at www.nlr.gov/publications

is not in use before transmitting a message. Generally, two heliostats should not be attempting to communicate at the same time over the same frequency as an HCUCC sends a downlink only after receiving an uplink from the tower. In other words, frequencies in use by each heliostat are fully synchronized by the tower. Additionally, messages are tagged with a time-to-live tracking to discard messages exceeding their time or hop limit if applicable.

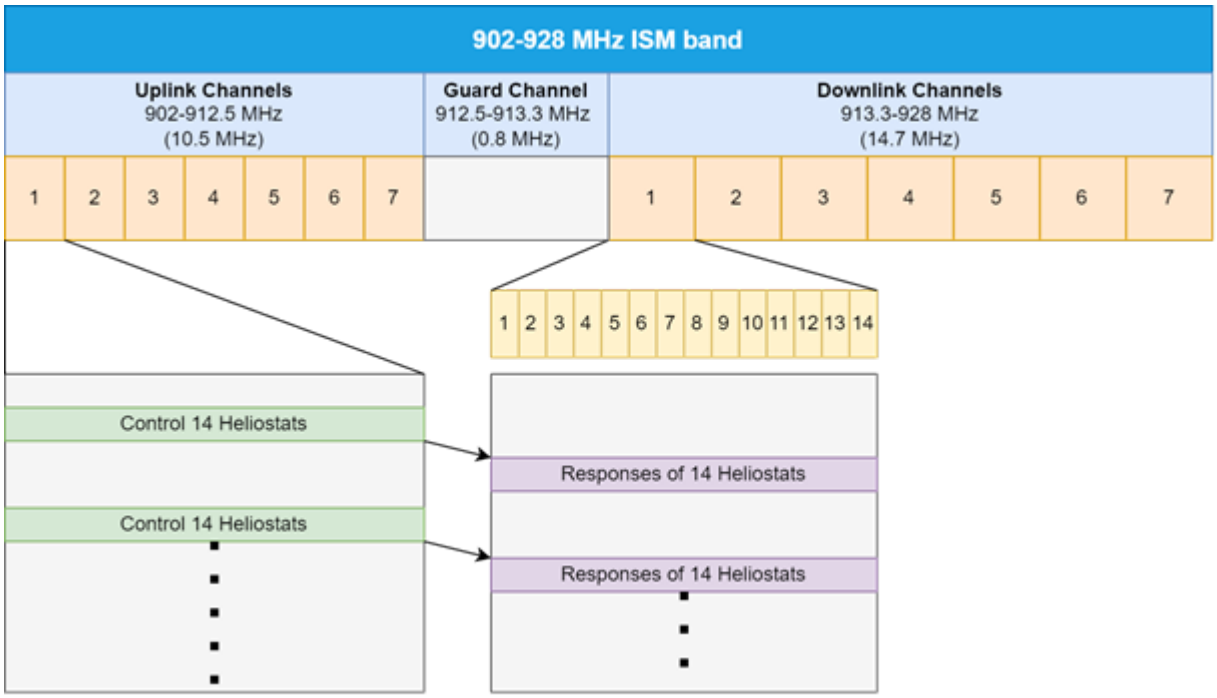

Figure 11. An example of the spectrally dependent uplink and downlink channels for the 915-MHz ISM band.

Note here 14 heliostats are shown per jumbo frame as an example, but 16 heliostats per jumbo frame are used at the Flatirons. Although the 14 downlink channels are grouped in a sub-band, each downlink is a separate message.

4.1.3 Design for Heliostat Field Size and Communication Rate

The heliostat field size for the 915-MHz band depends on the desired communication rate. If a 1-Hz communication rate is targeted (all heliostats communicated with in 1 second), calculations for the uplink and downlink channels are as follows. For the uplink channel: One jumbo frame requires 1,200 bits; at 1 Mbps, this results in 1.2 milliseconds per jumbo frame. Using 1.5 milliseconds to be conservative, this means 666 jumbo frames can be sent in 1 second. With 16 HCUCCs per jumbo frame, this means communication with 10,656 HCUCCs are possible per uplink channel in 1 second. Seven uplink channels equates to 7 * 10,656, or 74,592 heliostats. Note that in the setup at the Flatirons, one HCUCC is used for transmitting from the TCU, where 7 HCUCCs (or a more advanced SDR) can be used to transmit in parallel to achieve approximately 75,000 heliostats.

The downlink for a single heliostat/HCUCC requires 32 bytes or 256 bits. At 100 kbps, this is 2.6 milliseconds, or 3 milliseconds to be conservative. This results in 333 heliostats messages being sent in 1 second, where 16 heliostat messages can be sent in parallel over one downlink channel. Again, there are 7 downlink channels for a total of 16 * 7 * 333, or 37,296 heliostats per

This report is available at no cost from the National Laboratory of the Rockies (NLR) at www.nlr.gov/publications

the downlink side. Note that testing at the Flatirons uses a CaribouLite as the SDR, with the lower band channel configured as the ~2-MHz band parallel receiver. Alternatively, the system has been designed at scale for the USRP B206 mini, which has a maximum operational bandwidth of 56 MHz (planned operation in both the 915-MHz and 2.4-GHz bands), substantially more than the 14.7 MHz for 7 downlink channels. This SDR will improve substantially the amount of operational channels.

In summary, in the current design, the system is limited by the downlink side, which can handle approximately 37,000 heliostats at 1 Hz. If faster communication rates or larger heliostat fields are desired, then operating at the 2.4-GHz ISM band expands to 22 parallel downlink channels, opening up a factor-of-3 increase in field size or communication rate.

4.1.4 Other Features of Wireless Architecture

4.1.4.1 Network Node Acquisition

When turning on a TCU or powering up a node that is expected to operate within an existing TCU network, each node is automatically adapted into the network. This includes (1) being detected, (2) being configured, and (3) operating and being monitored. A TCU is periodically sending out beacons over uplink channels. The beacon contains Tower ID, software, hardware, and protocol versions, tower status, temperature, time, tower geo-location and network frequency channels (acquisition channel and Rx channels). During a configurable period, an acquisition channel is banned from usage by other active HCUCCs. When a new node receives a beacon, it is already programmed with the network parameters and tower properties; it knows its location, radio frequency (RF) time delay, and current wall clock time. The new node or HCUCC responds over the acquisition channel with its properties and the request to enter the network. The acquisition message is transmitted after an LBT sequence. Once the TCU receives the acquisition message, the HCUCC data are checked. If correct, the HCUCC enters the network and operation, and monitoring is then ongoing. Figure 12 provides an example of how beacon signals are periodically sent and heliostat data response channels and acquisition channels are allocated.

This report is available at no cost from the National Laboratory of the Rockies (NLR) at www.nlr.gov/publications

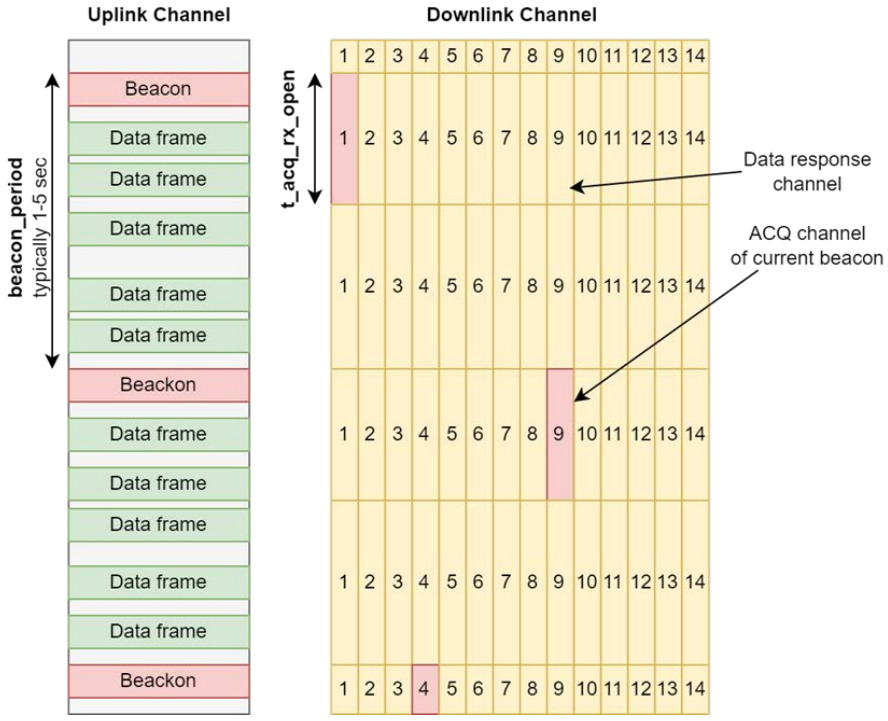

Figure 12. An example of periodic beacons being sent over an uplink channel to provide for network node acquisition

4.1.4.2 Tower Control Unit Transmission Power Adaptation

The TCU has an achievable transmission power variation of about 40 dBm. The goal is for each HCUCC to receive TCU signals with near the same power levels, but without power adaptation, HCUCCs that are farther away or near obstacles will have a reduced received signal strength. The TCU computer knows the location of each heliostat and assesses the expected path loss from the tower. This information is gained from geographic distance and the received signal strength of a nondeferred message from the tower. In all downlink messages, heliostats or HCUCCs include received signal strength from the last transmission received from the tower. The tower then uses this information to adapt and control uplink signal strength as needed.

4.1.4.3 Firmware Update Algorithm Updates Over the Air

The firmware update algorithm was not implemented in this work because of lack of time for completion and full testing of the code. Multiple firmware updates were applied to the Flatirons field, but each of these was achieved by a hardwire connection between a laptop and each HCUCC. Caribou Labs designed the FOTA algorithm scaffolding as follows. The TCU may issue a "firmware update start command," in which all heliostats receive a "FOTA" state transition command. The "firmware update start command" is followed by acknowledgment messages from the heliostats. Following this command, all heliostats are waiting for data.

The data structure contains chunks of information that are transmitted in a sequential manner in 256 byte chunks. Chunks are meshed (retransmitted) by some of the HCUCCs to allow for safe

This report is available at no cost from the National Laboratory of the Rockies (NLR) at www.nlr.gov/publications

and validated delivery to the geographically furthest HCUCCs. As the transfer is finished, the tower performs a "firmware update end command," after which all heliostats calculate the hash value or digital fingerprint of their received data and return it to the tower. After a verification sequence, the TCU commands the field to continue operation or reboot with the new firmware version. Although the data transfer protocol is relatively simple and could have easily been implemented, more development time and vetting are needed to ensure HCUCCs can default to a previous version of firmware in the event of an error or bug in a new version of firmware. It is critical to be able to always default to reliable firmware; otherwise a FOTA command could result in losing communication with tens of thousands of HCUCCs (requiring costly manual interactions to restore communications at each physical heliostat).

4.1.4.4 CLER Introduced

Digital signal processing (DSP) block libraries exist for programming SDRs to handle items such as time synchronization implementation of signal modulation. A significant portion of Caribou Labs' work was focused on software development for the TCU software defined radio to achieve the planned wireless architecture. It was expected that existing DSP libraries would be able to be used within the SDR code, but it was found that existing code was too heavy for embedded system use. Caribou Labs developed CLER, a new open DSP library that is lightweight and built for embedded devices. (CLER has an executable size and memory usage that is approximately 100 kilobytes (KB) instead of megabytes (MB) for existing options.) Figure 13 provides a comparison between CLER and various nearest options. With the completion of the development of CLER, Caribou Labs also demonstrated GMSK demodulation per the SDR. GMSK is an efficient digital technique that uses a continuous-phase frequency shift keying method to transmit data. Figure 14 shows a signal that was sent via the SDR with 31 embedded messages, where 100% of the bytes were correctly detected.

Feature	GNURadio	FutureSDR	LuaRadio	CLER
Language	Python/Cpp	Rust	Lua	Cpp 20
Software Spec	Framework	Framework	Library	Library
Frontend	Yes	Under Construction	No	No
Executable Size	~50MB	~5-15MB	~5MB	~100KB
Memory use	~100MB	~20MB	~5MB	~100KB
Embedded Devices	No	No	Yes	Yes (can be completely static!)
Threading	Multi-Threaded with built in Scheduler	Multi-Threaded with built in Scheduler	Single Threaded	Single / Multi Threaded
Block Definition	New Library and Multiple Files	Closure	Struct + Method	Struct + Method
DataTypes	Float/Complex/Byte/Int/ Short + PMT	Generic	Float/Complex/Byte	Generic
Speed (Est.)	Reference (1.0)	1.1	0.3	0.9
License	GPLv3	Apache 2.0	MIT	?? (MIT Liquid + MIT SPSC-Queue)

Figure 13. Comparison of CLER, an open-source DSP library for the SDR, versus existing software that was not going to work for the SDR at the Flatirons

This report is available at no cost from the National Laboratory of the Rockies (NLR) at www.nlr.gov/publications

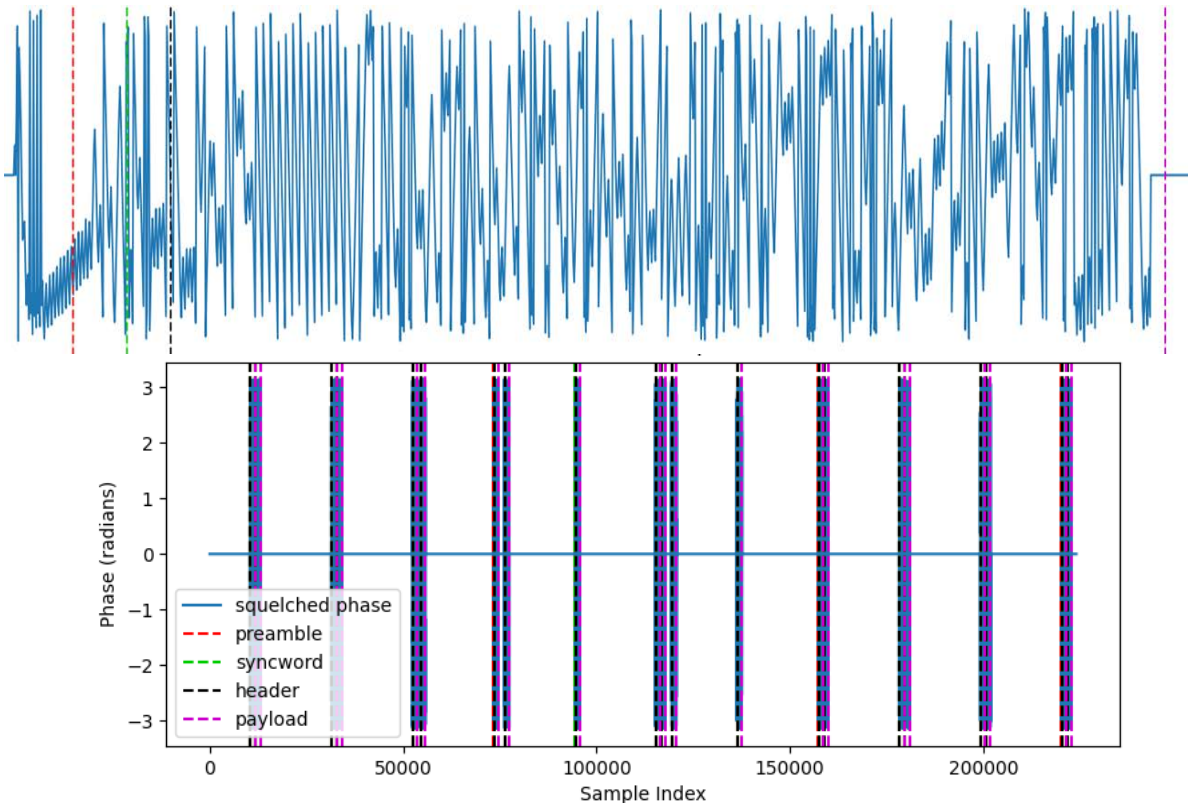

Figure 14. The upper image shows a signal sent with GMSK (time verse frequency), and the lower image shows a breakdown of extraction of message parts.

Thirty-one messages were sent, and 100% of the bytes were detected correctly.

4.1.5 Cost Breakdown

The appendix provides a complete table of the parts, including testing, and assembly for the HCUCC. The parts are priced from Mouser Electronics (a common worldwide electronics supplier) as of May 2026 at a quantity of manufacturing 30,000 HCUCCs. The total per HCUCC is $26.56. This version of the board is not necessarily cost optimized, and Mouser is not necessarily the lowest-cost electronics supplier.

4.1.6 Flatirons Field Test Layout

Figure 15 provides a map of the 100-node layout at the NLR Flatirons campus. The distance between node 1 and node 100 is approximately 900 m. The map shows that the test area of the Flatirons campus also includes several photovoltaic systems (these are approximately 2–3 m high) as well as a handful of wind turbines and other industrial equipment. The layout was chosen to work within available test space (many other projects exist at the Flatirons) while grouping some HCUCCs in clusters and achieving near 1 km of maximum distance across the field. Figure 16 shows the mounting of the TCU box and the receiving and transmitting antennas on the meteorological tower, while Figure 17 shows the TCU location in relation to the ground (roughly 30 meters high). Figure 18 shows an example of mounting of one of the HCUCC enclosures on a steel post (about 1.3 m high).

This report is available at no cost from the National Laboratory of the Rockies (NLR) at www.nlr.gov/publications

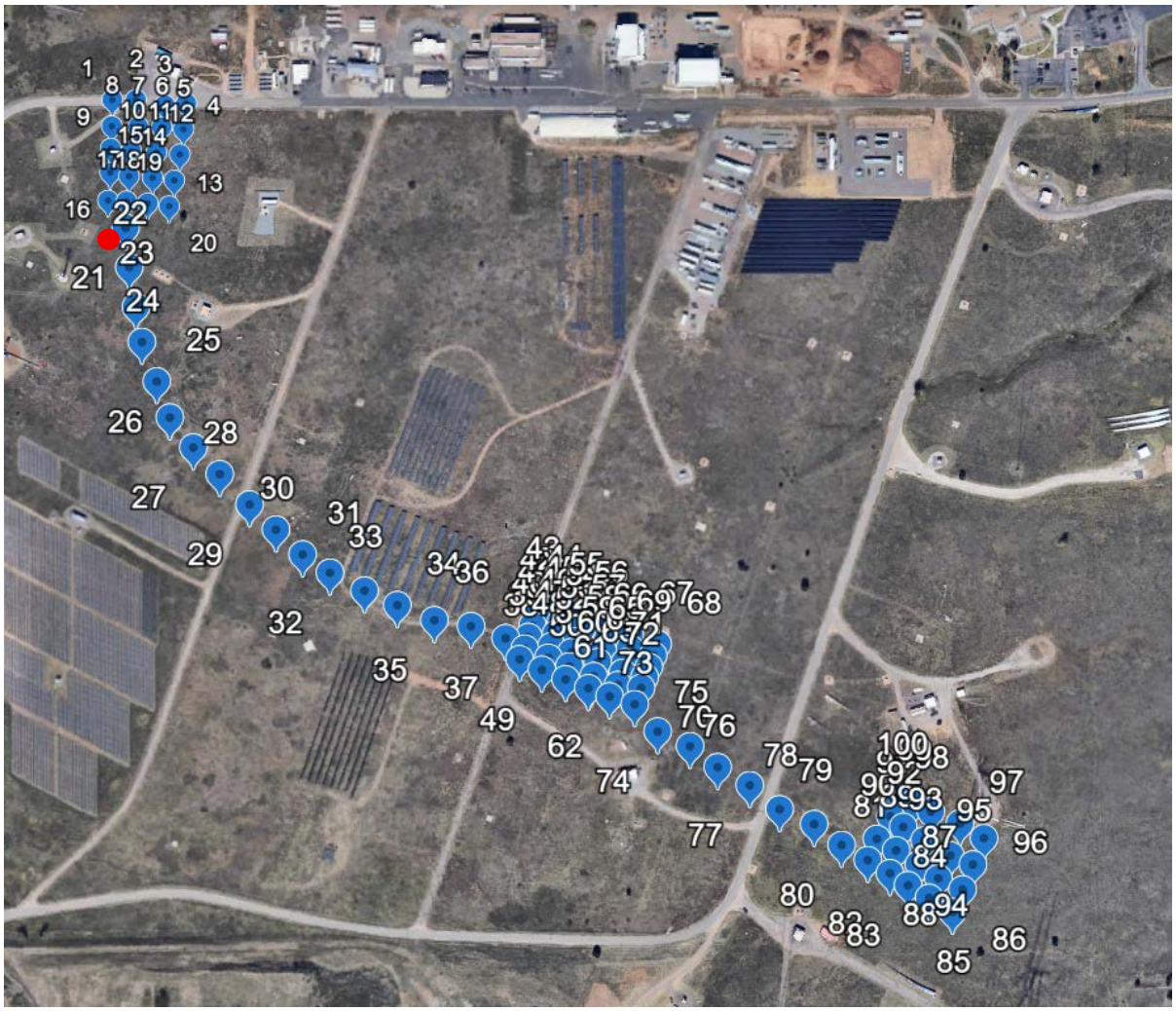

Figure 15. Satellite map of the Flatirons campus with overlay of 100 HCUCC nodes.

The TCU is located on a meteorological tower to the left or west of node 21 marked with a red dot.

This report is available at no cost from the National Laboratory of the Rockies (NLR) at www.nlr.gov/publications

Figure 16. Mounting of the TCU enclosure and transmitting and receiving antennas on the meteorological tower to the west of node 21

This report is available at no cost from the National Laboratory of the Rockies (NLR) at www.nlr.gov/publications

Figure 17. TCU is mounted ~30 meters high

This report is available at no cost from the National Laboratory of the Rockies (NLR) at www.nlr.gov/publications

Figure 18. One of the HCUCCs mounted in their outdoor enclosures at approximately 1.3 meters high

4.2 Simulation of the Flatirons Field

A network stack simulation was generated for RF channel emulation, the MAC layer, and cipher/cybersecurity algorithms. A block diagram for the RF channel emulation is shown in Figure 19, where the emulation is a complex structure to emulate RF path losses, bit-error-rates (BERs), SNRs, and received signal strength indicators (RSSIs).

This report is available at no cost from the National Laboratory of the Rockies (NLR) at www.nlr.gov/publications

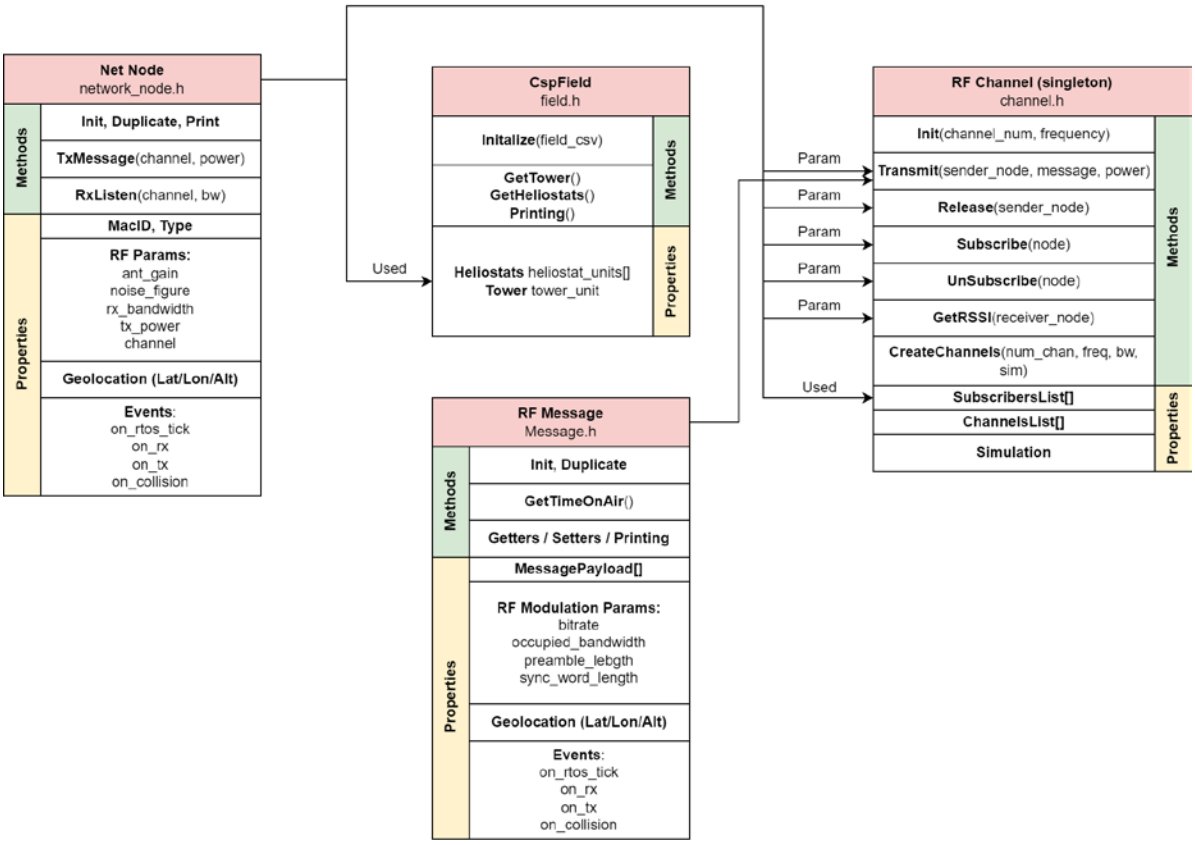

Figure 19. Block diagram for RF channel emulation

The network node block in Figure 19 is a basic unit that defines a node, which can be a tower or a heliostat. Network nodes have an "event-driven" mechanism and can subscribe into a channel and unsubscribe from it. Nodes can transmit a channel and can get the current RSSI on the channel. The RF message block in Figure 19 is the basic transmitting/receiving raw message that occupies the channel. It is defined by the sender and is delivered to the subscribers on the channel. It contains the modulation properties (bit rate, occupation time and data length) and contains the payload data bytes. The RF message gives the occupancy time on the channel that is primarily used by the channel simulator. The RF message object can vary so that different types of modulation are introduced, each with different properties. Currently GMSK modulation is emulated, which is what is being used in the Flatirons test field. The RF channel block in Figure 19 is the "message-routing" mechanism within the simulation. It contains subscriber nodes according to their geographic location and calculates the message delivery timing (according to path distance and speed of light), and the delivery power (RSSI) according to the path distance. It also introduces BERs and embeds them within the raw messages to emulate data losses. Terrestrial thermal noise is used in the SNR calculation where SNR_{dB} = Received Signal Level (dBm) − (−174 + $10\log_{10}B$ + NF), with B representing the bandwidth in Hz and NF being the noise floor. The BER is approximated as 1/2e ^ (−SNR/2). The time of propagation uses the geo to cartesian conversion in the GeographicLib library, while the path-loss calculation is a weighted average of the "ITU-RP1546," the "Log-Distance," and the "Two-Ray" Models (all industry standards). The CSP-Field block in Figure 19 encapsulates the field-level state. This block reads node locations and parameters from a CSV file and puts every field element in place.

This report is available at no cost from the National Laboratory of the Rockies (NLR) at www.nlr.gov/publications

This object is a “Field-Factory,” and once it finishes the “field construction,” it does not have an active role in the simulation. The running simulation is organized per the diagram in Figure 20.

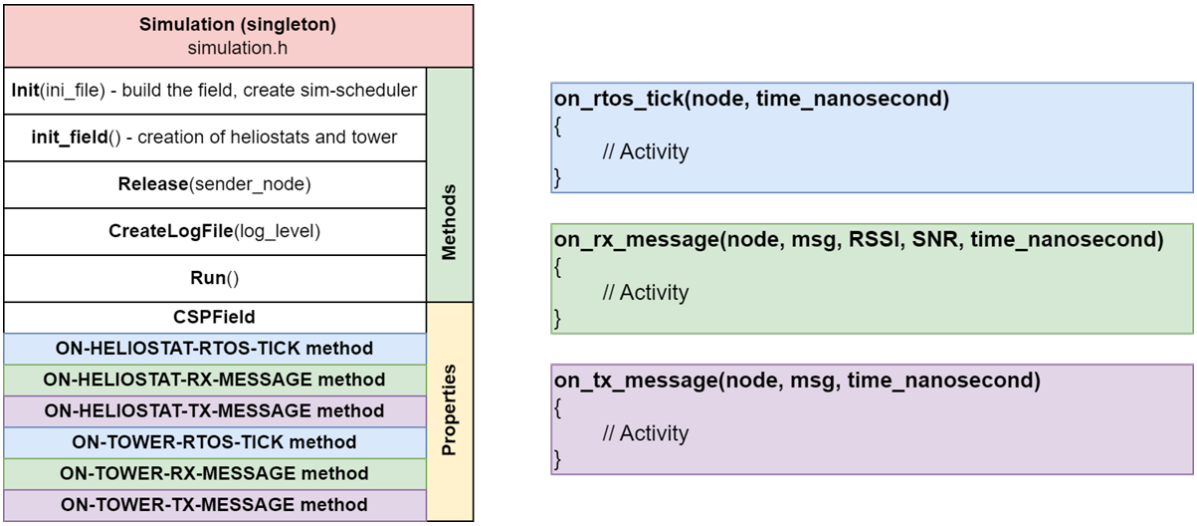

Figure 20. The organization of a simulation run

4.2.1 Simulation Results

The simulation was run to match the field layout provided in Figure 15 with 100 HCUCCs and one TCU. MAC layer encryption and decryption was incorporated with the RF emulation, as shown in Figure 21.

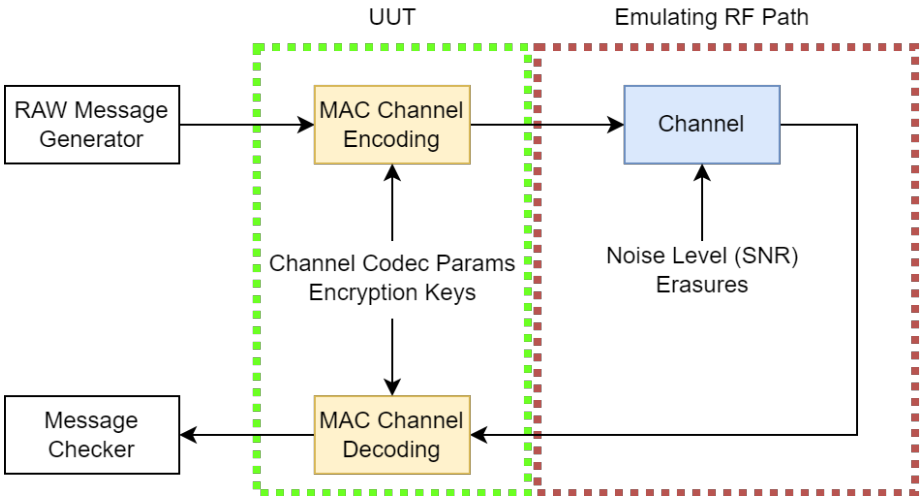

Figure 21. MAC layer encryption as incorporated with RF emulation

The simulation included 10^5 steps with MAC messages generated with: length = [30, 210] bytes, random variation of error correction parameters, and random variation of encryption keys. Channel emulation included Gaussian additive noise, injected random bit errors (up to 20 bit-switches per message), and injection of burst errors (up to 2 bytes erasure).

This report is available at no cost from the National Laboratory of the Rockies (NLR) at www.nlr.gov/publications

All results were logged into a CSV file, which can be loaded into Python for analysis and visualization.

The use of different numbers of parity bits in Hamming, (7,4), (15,11), and (31,36), were examined, as shown in Figure 22, for uplink messages and Figure 23 for downlink messages. In uplink messages at the same packet error rate, the SNR can be up to 4 dB lower, with Hamming included (up to 4.5 dB lower for downlink messages). For both uplink and downlink messages, all levels of parity bits are sufficient for maintaining a negligible packet error rate if the SNR is above 6.

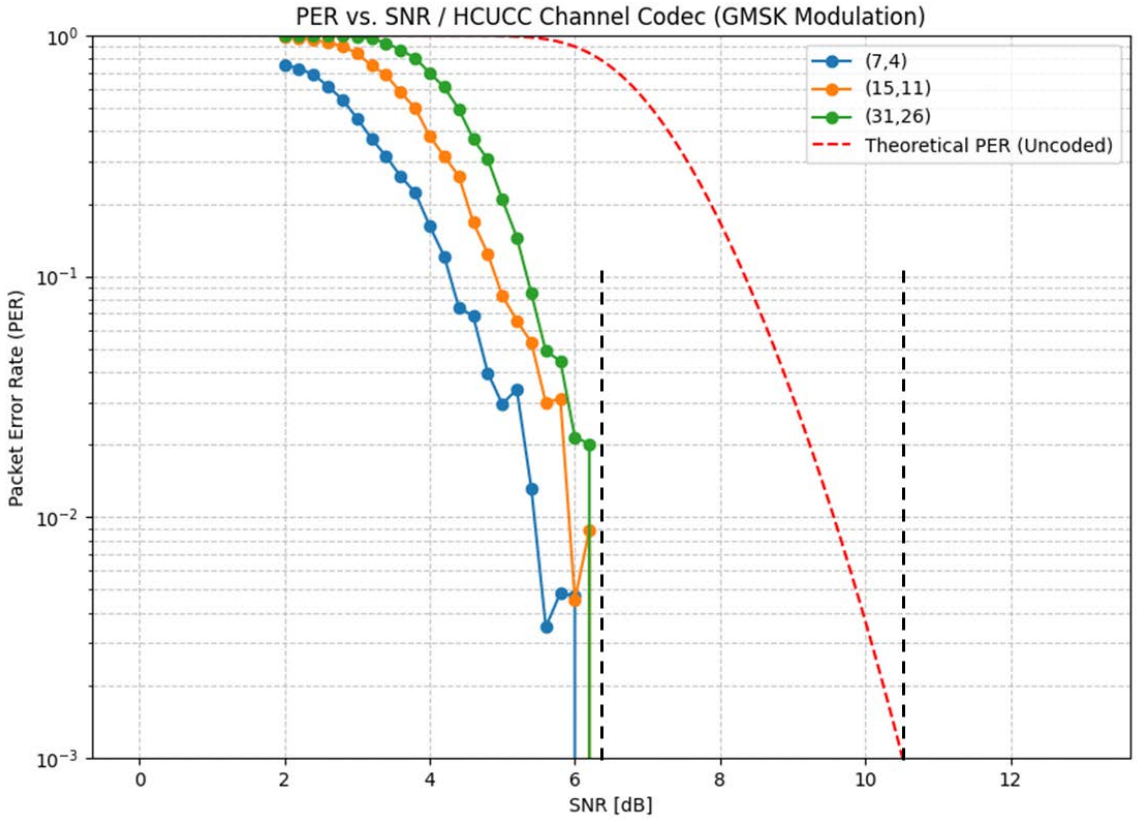

Figure 22. Results for coding and decoding uplink messages considering different parity bits

This report is available at no cost from the National Laboratory of the Rockies (NLR) at www.nlr.gov/publications

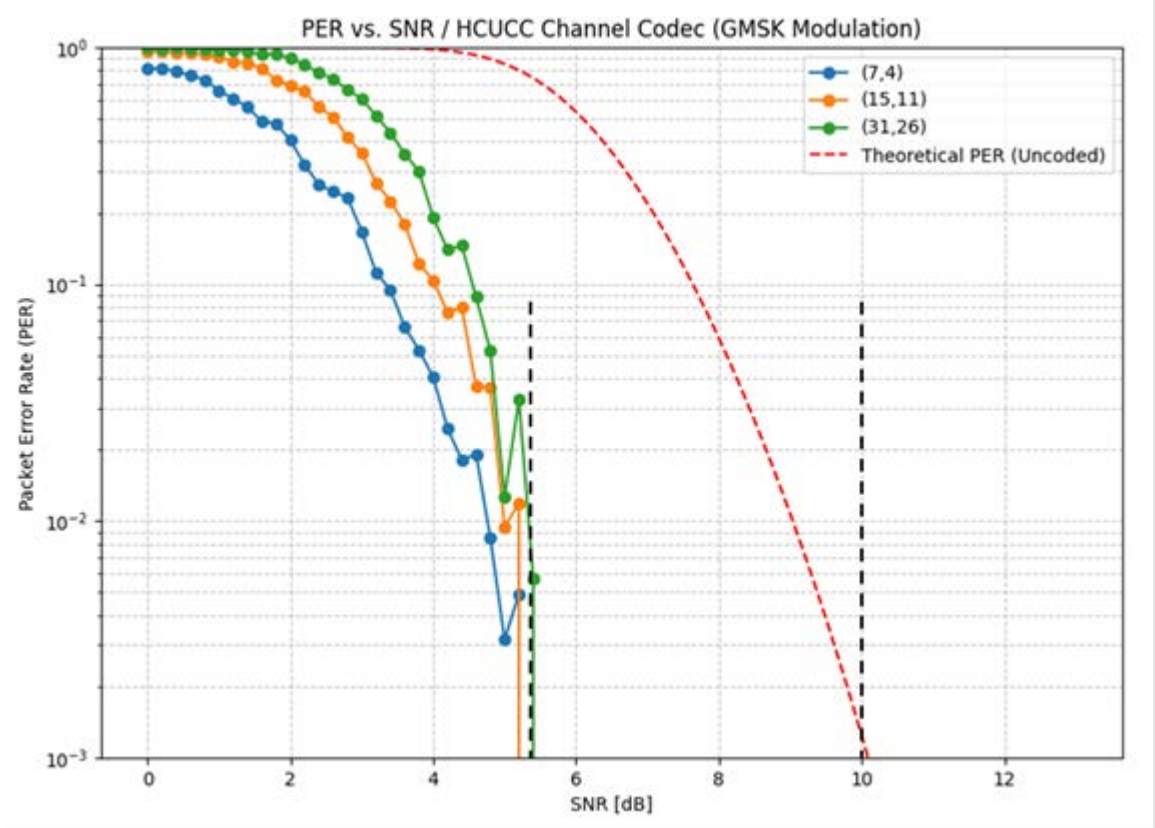

Figure 23. Results for coding and decoding downlink messages considering different parity bits

The simulation was used to examine CRCs for uplink messages (with good SNR) while varying the length of erasures in the message. Figure 24 shows the influence of 6, 8, 10, and 12 redundancy bytes. CRC8 or 8 bytes was chosen as it allows up to 4 bytes or consecutive erasures (~400 microsecond of channel blanking). Messages were also simulated with 1–2 bytes of erasure and up to 30-bit bitflips. This scenario emulated the possibility of long message transmission in the presence of a consistent jammer. In this extreme jamming case, greater than 90% of the packets were successfully recovered. The key performance indicators from the simulation are shown in the results section in Table 1 in comparison to field testing results.

This report is available at no cost from the National Laboratory of the Rockies (NLR) at www.nlr.gov/publications

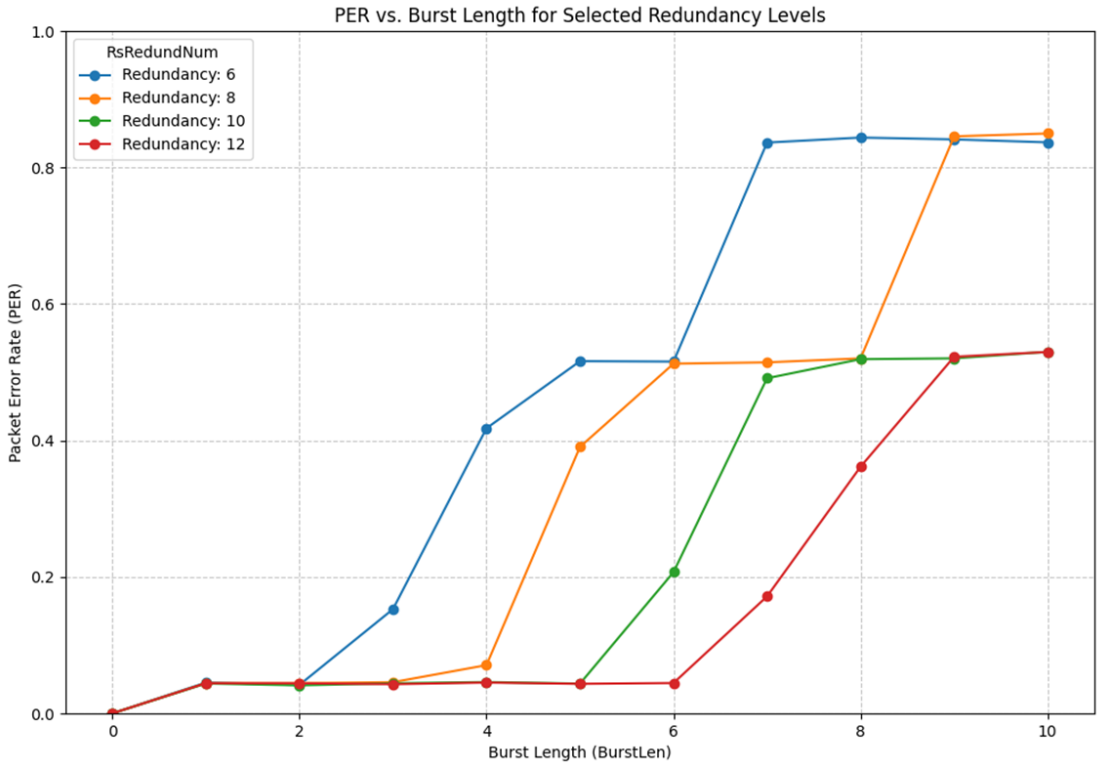

Figure 24. The simulated package error rate for different burst lengths and redundancy levels

4.3 Benchtop Testing and Initial Field Installation and Troubleshooting

Each HCUCC was benchtop tested for power up and node acquisition from the TCU, but the 100 nodes were not simultaneously tested for node acquisition and monitoring in the benchtop configuration. Although this was originally intended, because of late delivery of the full SDR software, the decision was made to move forward with Flatirons deployment of the TCU and the first 10 HCUCC nodes to achieve 60 days of field data collection before the project's end. Similarly, the HCUCC battery and solar charging hardware were subjected to an abbreviated validation test. In this case, a small number of HCUCCs and their charging units were deployed outdoors at NLR's main campus and basic functionality were confirmed. Some problems were found and corrected (e.g., certain LEDs were bypassed on the HCUCC to lower overall power usage), but field deployment was implemented without a multiweek outdoor test that is typical for this type of hardware. Additionally, the outdoor power testing did not include communication with the TCU. The HCUCC's software is designed to control the hardware so that when not in the relative high-power transmitting/receiving state, a sleep or low-power mode is enabled. By skipping testing of the power system without the TCU in the loop, the impacts of the software and the duty cycle (transmitting/receiving high power to low-power sleep) were based on calculations rather than validation.

The decision to move forward with the Flatirons deployment with less than the desired benchtop validation did not prove to be effective in accelerating overall system data collection. Data collection started, but immediately there was a problem in that not all 10 units were successfully

This report is available at no cost from the National Laboratory of the Rockies (NLR) at www.nlr.gov/publications

transmitting back to the TCU. Troubleshooting this problem and others in the field proved to be inefficient compared to the planned benchtop testing (the Flatirons is remote for the test engineers and winter weather conditions disrupted work on various occasions). After evaluation, it was deemed likely that those units not being received by the tower were due to their locations on the outside edges of the TCU directional transmitting and receiving antennas. Additional HCUCCs were added to the field, but not all of the new units were heard by the TCU, even though the new units were well within the directional pattern of the antennas.

Physical hardware examination of each of the units not being heard and data from functioning units indicated various problems: (1) HCUCC software errors, (2) HCUCC antennas not performing as expected while inside their enclosures, and (3) in some units low battery charge state. A cycle of correcting the various issues and retesting took multiple weeks that likely would have taken days if an outdoor benchtop setup had been instituted at NLR's main campus. This was because of remote and weather challenges associated with the Flatirons and the fact that, without FOTA capability and with HCUCC's spread over a large field, engineers had to walk to each unit with a laptop to make multiple software updates.

The simple lesson is that when building a wireless communication network such as this, outdoor benchtop testing with all nodes in close proximity must demonstrate that all nodes can successfully communicate for multiple hours with the TCU and that the majority of the nodes can communicate successfully over at least 2 weeks before expanding to a large field. The 2-week test should also include taking several units to the low battery charge and demonstrating recovery of full charge after a designed number of sunny hours. If cloudy weather does not occur, low charge state can easily be achieved by covering the solar panels on certain units. As a result of skipping the in-depth power system test, a serious problem was not found on the charging hardware until after more than 40 HCUCCs were installed in the field. There was no possibility of correcting the defective board components within the remaining project timeline, and therefore an off-the-shelf Adafruit solar battery charger board was purchased and installed in the field.

Correcting software bugs and adding new solar chargers increased the number of units that were successfully communicating with the TCU, but there were still missing units that were clearly the result of transmitting and receiving signal issues. Investigations altering the HCUCC antenna orientation and mounting proved that missing HCUCCs could at least be temporarily brought online. Simulation results and expectations of signal strength based on calculations for the antenna hardware and power suggested the tower should be receiving the messages regardless of field position. Investigations with a portable spectrum analyzer showed unexpected 915-MHz signals present at the Flatirons campus. The tower was set to work as a spectrum analyzer to gather all spectral signals heard in the 915-MHz region while communication to HCUCCs was ongoing. Figure 25 shows one chunk of spectral data collected by the tower SDR. The high levels of interference suggested the tower could be missing messages from some of the HCUCCs because other stronger signals were heard in the same frequencies of the missing HCUCCs or LBT could be preventing the HCUCCs from sending downlinks.

This report is available at no cost from the National Laboratory of the Rockies (NLR) at www.nlr.gov/publications

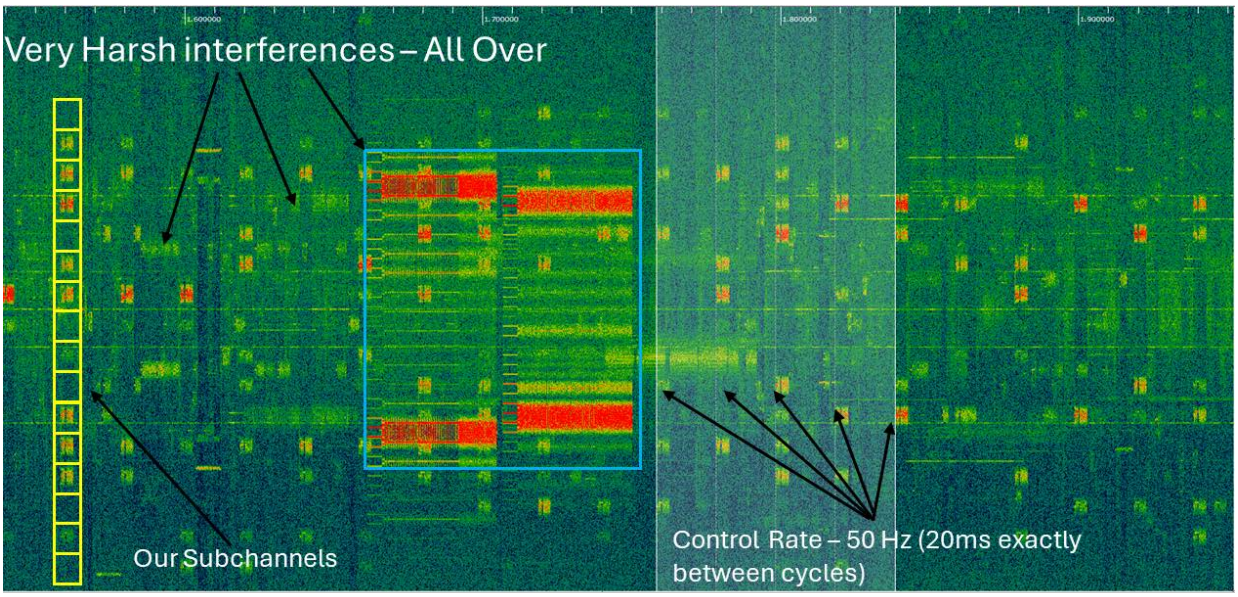

Figure 25. Spectral data in the 915-MHz band collected using the tower SDR shows that there are large amounts of interference from other ongoing communication at the Flatirons.

The area boxed in blue shows a signal not coming from HCUCCs that is near the maximum use of the time domain.

Figure 26 provides an additional example of spectral data in the 915-MHz band collected by the tower SDR, where annotation shows communication per FSK, LoRa, and PSK/QPSK (none of which come from HCUCCs).

Changing antenna location within some HCUCC enclosures served to boost downlink from the HCUCC. In some cases, this increased the number of active nodes that could be heard within the existing interference by the TCU. Physical testing of antennas while monitoring HCUCC status LEDs indicated the most likely problem was that certain HCUCCs were not receiving their messages from the tower and then were staying silent (rather than the tower not hearing HCUCC messages among the site interference). In all observations, once the HCUCC receiving LED came on, the transmitting also came on, and the given unit was also heard at the tower. Further testing is needed, but observations point to problems with HCUCC antenna or antenna configuration (the antenna orientation, connections, or shielding by the solar cell on the lid of the enclosure) rather than field interference. If the problem HCUCCs antennas were sufficient to receive the uplink without interference, then it is to be expected that these HCUCCs would be heard at the TCU some of the time because of frequency randomization.

In practice, these HCUCCs were not heard unless adjustments to their antenna were made. With this knowledge, the remaining HCUCCs were installed as planned for the 100-node network while attempting to position each antenna to better hear each unit at the TCU. After antenna adjustment, more than 70 nodes could typically be heard by the TCU, 5 units were dead due to unknown hardware issues, and approximately 25 units still did not hear the tower unless the lid was removed from the enclosure. The following options were considered to bring the remaining units into regular communication as well as boost how often certain units were heard: (1) find the primary source of interference and pause it for a short-term test of 95 functioning nodes, (2) replace internal antennas with external antennas on select HCUCCs, (3) lower the TCU antenna

This report is available at no cost from the National Laboratory of the Rockies (NLR) at www.nlr.gov/publications

to potentially increase SNR, or (4) run spectral analysis at 2.5 GHz—and if less interference, make the software change to operate at that band. At this phase in the project (final quarter), partner Caribou Labs was not accessible, and therefore items 3 and 4 were considered unfeasible. Attempts were made to find the primary source of interference, but these were unsuccessful. One external antenna was tested on an HCUCC, but this test did not show significant impact, and therefore this option was set aside. The decision was made to collect data over 1 day from the currently communicating HCUCCs, analyze this data, and report on the findings within the remaining project timeline.

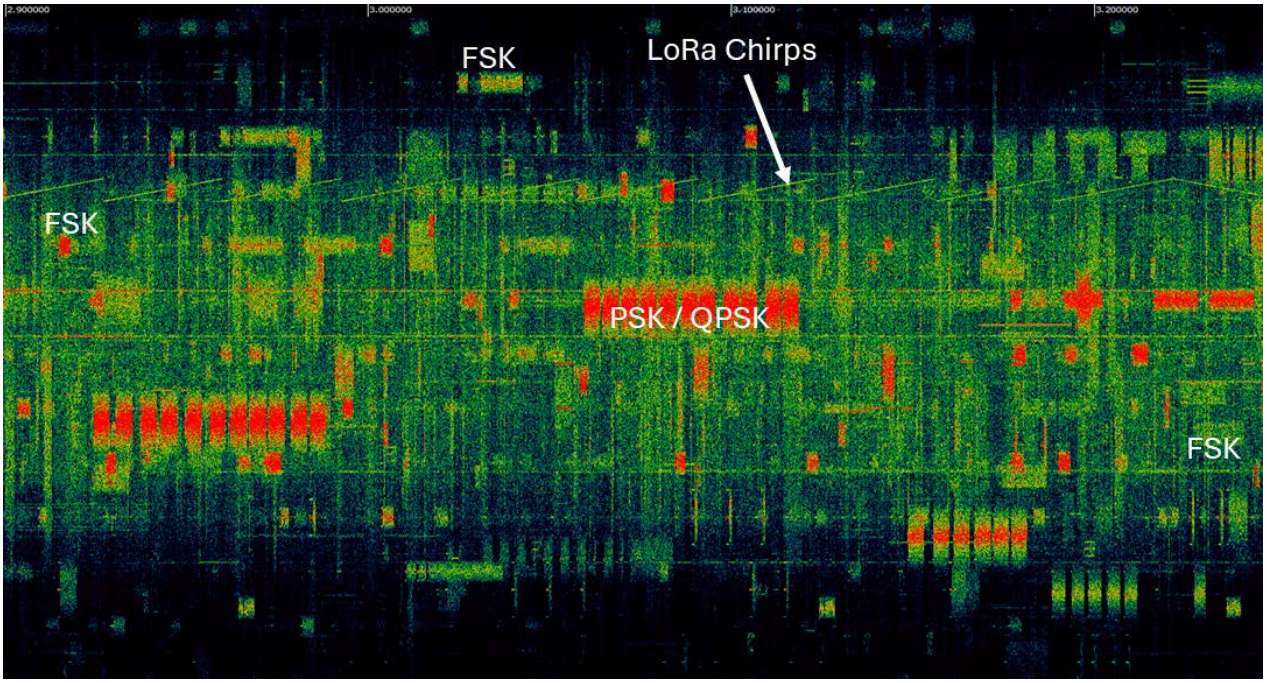

Figure 26. An additional example of spectral data in the 915-MHz band collected by the tower SDR highlights communication per FSK, LoRa, PSK/QPSK (none of which come from HCUCCs)

4.3.1 Data Collection and Results

On February 26, 2026, the system was run for approximately 5.5 hours, during which time a total of 83.8 million messages were sent from the TCU. Figure 27 shows the 74 heliostats (with a slant range spanning 167–908 m) that were actively communicating with the TCU during the data collection.

This report is available at no cost from the National Laboratory of the Rockies (NLR) at www.nlr.gov/publications

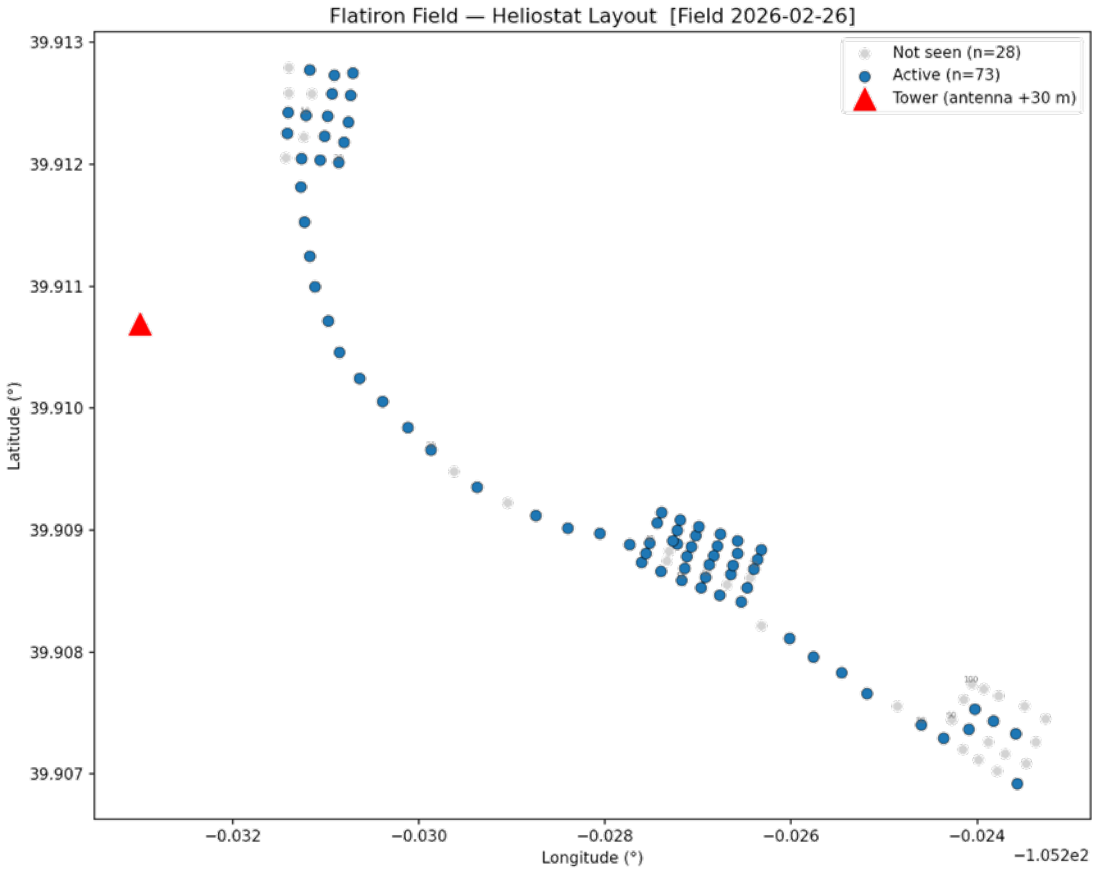

Figure 27. The figure shows the heliostats in dark blue that were active during the data collection on 2/26/26

Figure 28 shows the median HCUCC Rx power (dBm), while Figure 29 shows the median SNR (dB calculated relative to the noise floor), and Figure 30 shows the average response time in seconds. Table 1 provides key results from both the simulation and the field test data.

This report is available at no cost from the National Laboratory of the Rockies (NLR) at www.nlr.gov/publications

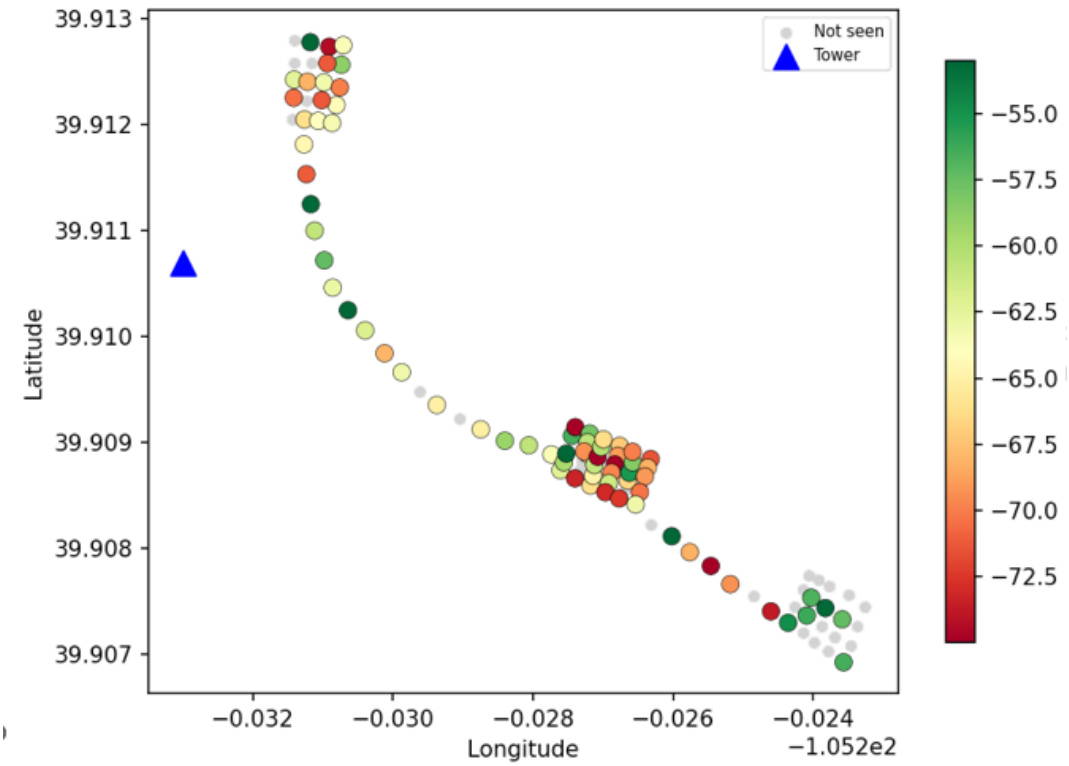

Figure 28. Median HCUCC Rx power in dBm

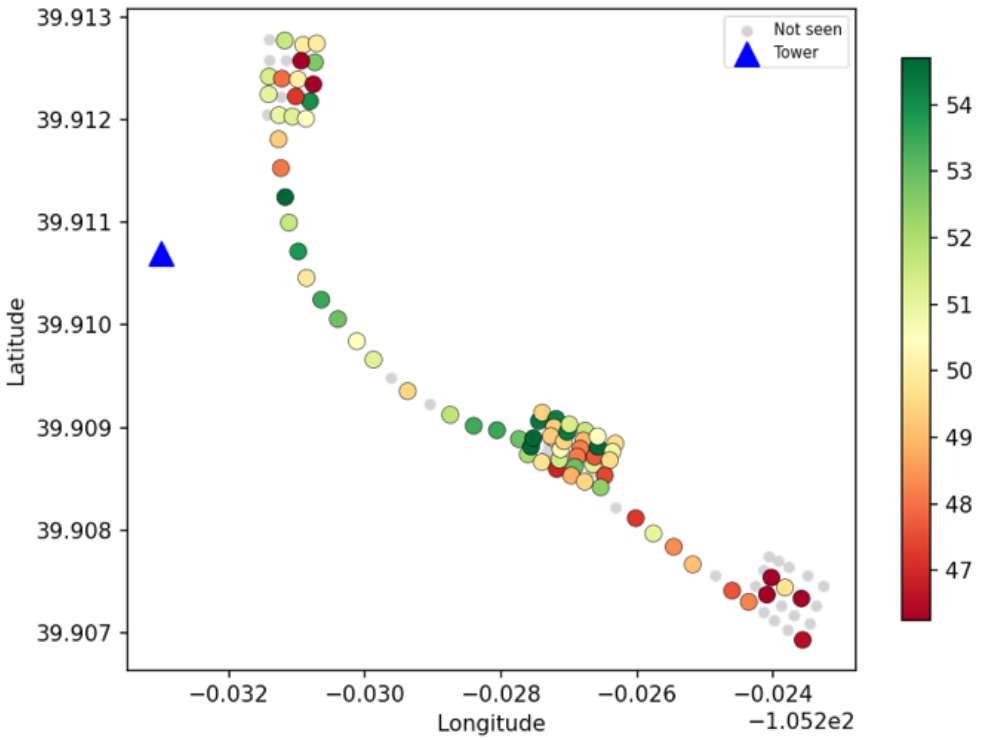

Figure 29. Relative calculated SNR in dB (power at the TCU Rx antenna minus the noise floor)

This report is available at no cost from the National Laboratory of the Rockies (NLR) at www.nlr.gov/publications

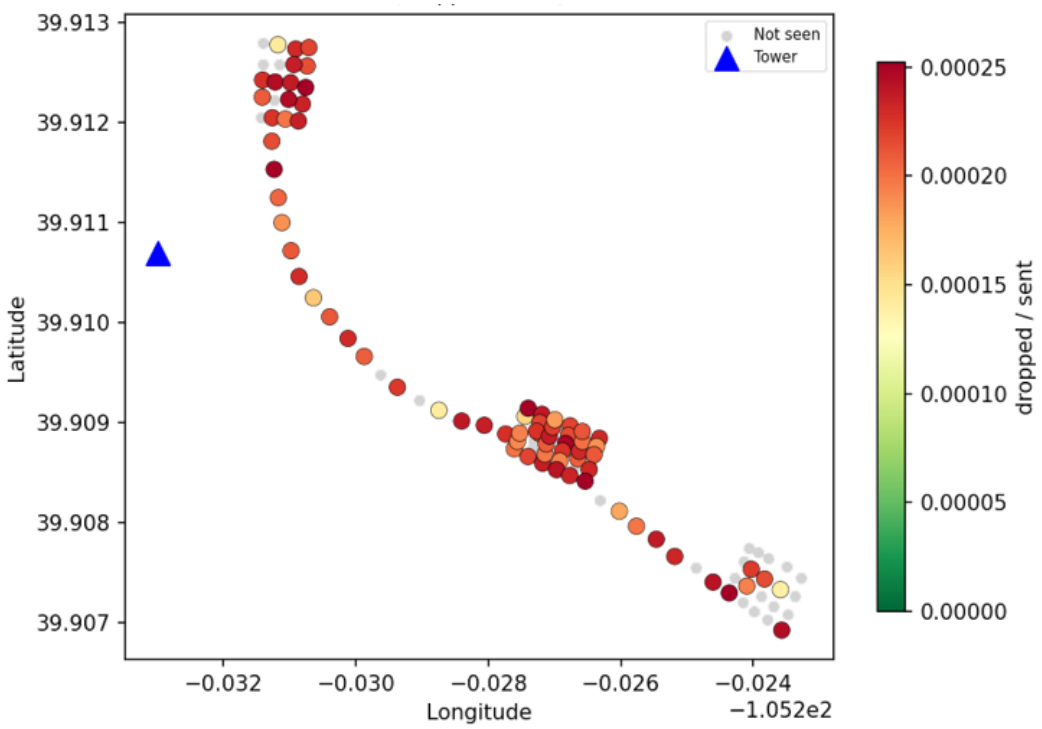

Figure 30. HCUCC message drop rate

Table 1. Key Results From Both the 100-Node Simulation and 74 Nodes in the Field

Metric	Simulation—Not Jammed	Simulation—Jammed	Field Test (Median)
Uplink SDR SNR	~31 dB	~16 dB	50.2 dB
Uplink RSSI at SDR antenna	−83 dBm	−83 dBm	−60.8 dBm
Average response time	6.33 ms	23.6 ms	21.2 ms
Response time std dev	0.18 ms	0.18 ms	10.9 ms
Control loop rate	10.41 Hz	9.6 Hz	24.0 Hz
Bit error rate	0	~0.1 (growing)	(*)
Dropped messages	0 / 350,000	Growing	0.20% (168k / 83.8M)

*Bit error rate values from field hardware are unreliable due to a firmware reporting artifact.

This report is available at no cost from the National Laboratory of the Rockies (NLR) at www.nlr.gov/publications

The field results show RSSI/SNR higher than simulated, where review of the simulation shows it assumed a larger field (~3-km scale due to a coding error), which accounts for the ~22 dB difference in RSSI (−60.8 vs. −83 dBm) and the elevated SNR. The link is effectively over-engineered for this field size. At 21 ms, the measured response time is close to the simulated jammed case (23.6 ms) rather than the clean case (6.33 ms). This could indicate retransmission overhead or protocol-level congestion rather than RF jamming, given that the RF SNR is well above the given threshold. The simulation assumed a moderately jammed channel, where the field shows significant interferences, driven by external systems protocol-level effects (scheduling jitter, collision avoidance, retransmissions). Message drop rate was acceptable: 0.20% total across 83.8 million messages, considering all data collection was occurring during what is similar to an extreme jamming attack. With the data that were collected, it is unknown if the dropped messages are on the uplink or the downlink side. Note that all wireless systems are vulnerable to jamming, while advanced systems use frequency hopping to avoid jamming frequencies. The full-scale Caribou Labs architecture includes frequency hopping. As noted, the planned SDR, the USRP B206 mini, has 56 MHz of operation bandwidth, and the system will be able to easily hop between the 914-MHz and the 2.5-GHz bands to be reliable even in a jamming attack.

4.4 Key Field Test Outcomes

There are further steps or improvements that will be made to the hardware and software under test, but the data collected demonstrate the overall architecture performs as expected. The results of this test field substantially de-risk the technology and support the calculations for scaling the technology to tens of thousands of heliostats while delivering encrypted sub-second communication. The hardware was designed to be producible using U.S. components, and at volume, the bill of materials is less than $30 per heliostat. All hardware is open-sourced and can therefore be easily adopted by heliostat manufacturers or CST field designers as part of hitting DOE heliostat cost targets of $50/m^2. Design and testing of a control stack framework was achieved, including software/network algorithms and security/encryption. A major DSP engine, “CLER,” was open-sourced by Caribou Labs and is already in use by others. Testing the system in a real field with significant interference provided direct understanding of the risks, experience with mitigation strategies, and a long list of lessons on how to efficiently approach moving to a production-level system.

4.5 Lessons Learned

4.5.1 System Power Supply and Consumption

As discussed, the battery and charging system were not sufficiently sized and tested for field deployment in NLR/Colorado winter irradiance conditions. An updated design will optimize the hardware and battery for at least 8 days of storage (minimizing power usage when not in transmitting/receiving mode) and must be validated with a longer-term outdoor operational period. The system enclosure will be increased in size to accommodate a solar panel that can recharge the battery over an 8-hour sunny period.

The chosen photovoltaic maximum power point tracking integrated component required the photovoltaic panel output less than 5 volts, which was overly constraining when considering

This report is available at no cost from the National Laboratory of the Rockies (NLR) at www.nlr.gov/publications

photovoltaic supply options. Alternatively, using TI BQ25638YBGR or a similar unified device opens up photovoltaic supply options while supporting power measurement, maximum power point tracking, and battery management. This component (or similar alternative) should be facilitated on the main board to seamlessly handle power management. There are several board power consumption issues that can be revisited and improved: DC-DC power conversion, maximum power point tracking methodology, removal of constant power consumers like indicator LEDs (useful in prototyping but not needed at full scale), removal or power gating the temperature compensated crystal oscillator (alternatively working with the raw quartz crystal component). Currently, when powered through USB, the device draws extra energy to power the USB chip (Cypress). This integrated component does not enter low-power mode by default. Additionally, the low-voltage power entry path goes through a power-hungry diode. Replacing it with a power path dedicated integrated component should be considered.

4.5.2 Manufacturing Concerns

The project encountered several avoidable development bottlenecks because of manufacturing too few units (120 for a 100-node network) and delivering hardware units to NLR too fast. Fifty percent more units should have been manufactured than the original 120. This would provide sufficient units for in-house development and gradual delivery to NLR as the software was more fully vetted. Caribou Labs had 25 units manufactured up front, but these were found to have a fake USB component and were scrapped. This manufacturing problem caused a significant time delay, and the next batch was pushed to the full 120 to be able to deliver to NLR per contract deadlines. As mentioned earlier, there were other board failures and problems with the battery charging system in the batch of 120 units. These problems further introduced delays and forced temporary patches to problems. It is recommended, while prototyping and testing, to manufacture small batches of 5 to 10 units that are subjected to a documented test protocol, including outdoor operation before producing more units. Scaling to larger quantities should not occur without confidence all is working per the full test protocol.

4.5.3 Hardware-Level Lessons

4.5.3.1 Main Chip

The Texas Instruments CC1352 is the integrated, multiband, and multiprotocol wireless microcontroller that allows operating in both the 915-MHz and 2.4-GHz frequencies. The component is very capable for its price and works above expectations. On the other hand, Texas Instruments' development and debugging tools are currently prone to issues and difficult to use. This issue needs to be considered when working with this chipset. On the other hand, Texas Instruments' RTOS is a very responsive and mature operating system.

4.5.3.2 Radio Frequency System

The natively provided 19-dBm RF power amplifier from the device is sufficient for the 1,500-m use case, but it could be valuable to provide the board with an additional power amplifier, which is gated and can be bypassed (this provides adaptability for greater distances and areas with interference). Consider adding a power amplifier for at least 27 dBm. Pros include an additional 8 dB of margins for link resilience; cons include higher power consumption (~2.5–3 times more,

This report is available at no cost from the National Laboratory of the Rockies (NLR) at www.nlr.gov/publications

on average), higher board cost, and additional complexity to the software and hardware. Performance of the antenna on the HCUCC side was evaluated in the design phase, but this evaluation excluded consideration for being inside a box with a solar panel on top (which requires being tilted and oriented for optimal irradiance collection). The optimization of the HCUCC antenna needs reevaluation in this context as well as full performance evaluation as assembled.

4.5.3.3 More Flexibility in the Development Stage

During the project we drew up (has not been printed and tested) an add-on expansion board for the HCUCC to directly connect the HCUCC to heliostat control hardware. It makes sense to support future iterations for this type of evaluation kit for research and experimentation. It also is practical for the research kit to have a larger battery because higher power consumption items like indicator LEDs are valuable in diagnostics and troubleshooting. Generally, this kit should have easier and accessible inputs and outputs on the HCUCC board. The usage of miniature Molex bottom connectors impeded fast-pace debugging and agility, and it may be valuable to replace them by a standard 0.1-inch connectors.

4.5.3.4 Radio Frequency Surveying and Tooling

By default, it was assumed that the Flatirons campus would not have problematic interference at the 915-MHz frequency band. A spectrum analyzer was rented for ~$500/month when problems occurred. At the beginning of the project, it should have been a requirement to survey both the 915-MHz and 2.4-GHz band in planning for deployment. A directional survey could have been conducted with the rented equipment or broad frequency analysis with the SDR as demonstrated in the project.

4.5.4 Software-Level Lessons

4.5.4.1 HCUCC Board Firmware

The benefits include a simple architecture that is C++-based, easy to adapt with configuration flow, and reusable as a platform. The cons include firmware development that is difficult with Texas Instruments' current ecosystem. In conclusion, the software should be adapted to open-source ecosystems. Multiple firmware updates were made as a result of bugs in the system. Field updates were time-consuming without FOTA, and therefore priority should be placed on completing and validating FOTA software.

4.5.4.2 Tower-Listener

The system was late in delivery because existing frameworks such as GNURadio proved to be problematic. Alternatively, the project provided the bonus of developing the open-source CLER Library, and the TCU proved to work well with CLER (see Other Features of the Architecture section). CLER provided a multichannel decoder fast enough to be facilitated even on a constrained hardware such as a RaspberryPi. Additionally, a wider-bandwidth SDR is feasible on such devices. Future testing should include the USRP B206 mini as it is intended at scale and its cost is not prohibitive.

This report is available at no cost from the National Laboratory of the Rockies (NLR) at www.nlr.gov/publications

4.5.4.3 Tower Application

The TCU works as expected, though improvements can be made on channel feature approximations, such as optimal subchannel selection based on spectral interferences. For now, because of a high level of channel clutter, we chose a random channel allocation algorithm, providing different HCUCCs equal chance to reside on a quiet channel. This stochastic method provides a good solution for randomly cluttered channels.

This report is available at no cost from the National Laboratory of the Rockies (NLR) at www.nlr.gov/publications

5 Next Steps

Next steps can be divided into two categories: (1) improvement and finalizing the existing system, which is estimated to require $100,000 to $150,000 to complete, and (2) creating a production-level system (off-the-shelf ready) that is estimated to require greater than $600,000 to complete. The left of Figure 31 shows a list of items needed to improve or fix the current 100-node network. There are software features like the TCU graphical output that currently report meaningless values that can easily be corrected to provide better system feedback. A more time-consuming software item is completing the code for FOTA updates and testing for resiliency to bugs in new firmware versions. Although this is time-consuming, it is critical to being able to rapidly make improvements to the HCUCC software. Improving the HCUCC power system and antenna mounting would allow the system to run as intended and capture long-term data in varying field conditions.

These long-term data are expected to provide fruitful information toward further optimizing the performance and spectral efficiency of the system. A bit error rate test should also be implemented in the process to accurately report on system performance. The right of Figure 31 provides an overview of the key items needed to achieve an off-the-shelf system for heliostat fields. There are obvious RF engineering hardware and software iterations needed to prove the system is robust and ready for seamless field deployment. These processes are well developed and require a predictable number of engineering hours to complete. Additionally, the cost associated with regulatory testing and approval are well known. Alternatively, meeting market needs is a more uncertain task. Although the wireless architecture in this project has great promise, it will only be adopted if the features and cost dovetail well with the market needs. With the exception of China, the market is very limited in terms of heliostat fields being developed. Lack of an active market to work with is currently a significant barrier to finalizing a field-ready product.

This report is available at no cost from the National Laboratory of the Rockies (NLR) at www.nlr.gov/publications

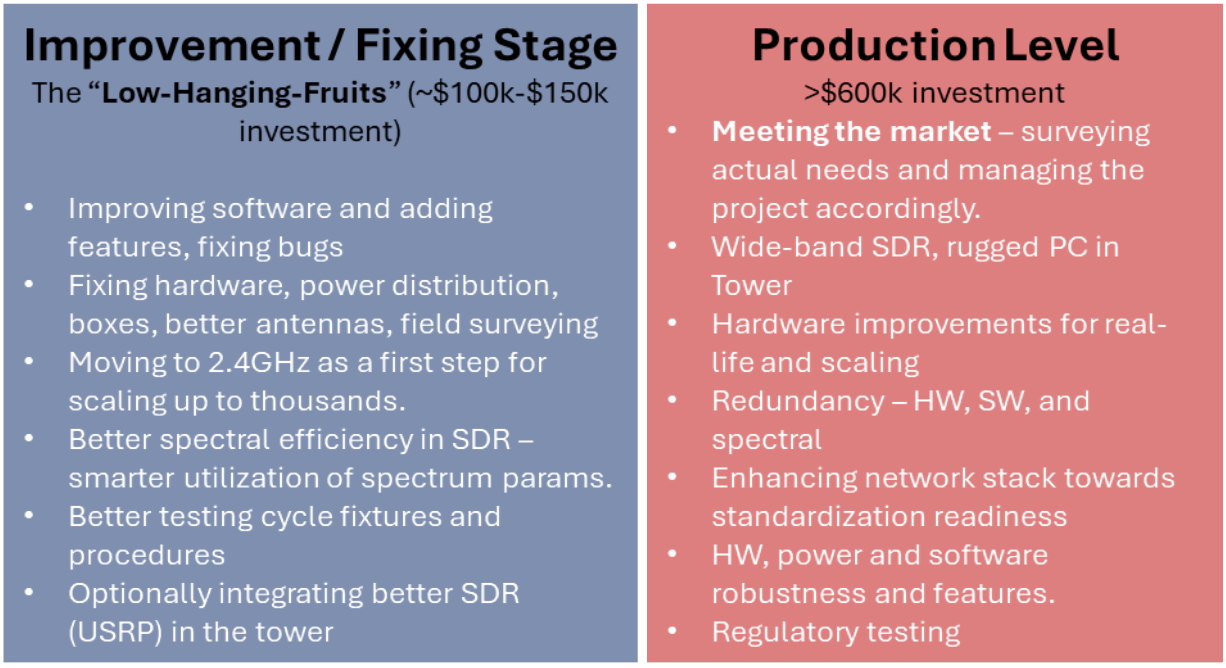

Figure 31. (left) Steps to improving/fixing the existing 100-node test bed. (right) Steps to developing an off-the-shelf system for the heliostat fields.

This report is available at no cost from the National Laboratory of the Rockies (NLR) at www.nlr.gov/publications

APPENDIX

Table A-1. Parts List and Associated Pricing for Printing 30,000 HCUCC Boards

Part Number	Qty	Unit Price $	Description
LXES1UTAA1-157	1	0.058	ESD Suppressors / TVS Diodes ESD Protection Device, 0402, Bidirectional, 4V working, 15V breakdown, 0.05pF Cd
AT25SF321B-SSHB-B	1	0.577	NOR Flash 32 Mbit, 3.0V (2.7V to 3.6V), -40C to 85C, SOIC-N 150mil , 108 MHz, Single, Dual, Quad SPI NOR flash
74HC4053BQ,115	1	0.190	74HC4053 - Triple 2-channel analog multiplexer/demultiplexer@en-us
M24C64-DRDW8TP/K	1	0.221	EEPROM 64-Kbit serial I2C bus EEPROM 105C operation, 200Yr retention, 1M Writes, 1.7-5.5V @2mA
BLM15HD182SN1D	6	0.017	Ferrite Beads 1800ohms GHz HiSpd
74438356033HT	1	1.180	WE-MAPI SMT Power Inductor, size 4020, 3.3µH, 3.6A, 51.8mO
PMEG60T30ELRX	2	0.086	60 V, 3 A low leakage current Trench MEGA Schottky barrier rectifier
D18V0L1B2LPQ-7B	3	0.051	ESD Suppressors / TVS Diodes General 15kV Cont., 20kV Air, 20Vw Protection PP DFN1006-2
FTSH-110-01-L-DV-K-P-FR	1	1.200	High Reliability Header Strips, .050"x0.50" pitch, 10x2, plastic shrouded with middle key
LSM6DSLTR	1	2.540	IMUs - Inertial Measurement Units CONSUMER MEMS
LIS2MDLTR	1	1.690	Magnetoresistive Sensor X, Y, Z Axis 12-LGA _2x2_
52991-0408	1	2.110	Molex B2B 40 Pos, 0.5mm pitch
LTST-C190KRKT	6	0.013	Red 631nm LED Indication - Discrete 2V 0603
CONUFL001-SMD-T	1	0.471	RF Connectors / Coaxial Connectors U.FL Straight Surface Mount Jack
CC1352P74T0RGZR	1	4.590	RF Microcontrollers - MCU SimpleLink Arm Cortex - M4F multiprotocol sub-1 GHz and 2.4-GHz wireless MCU integrated power amp, 704 KB flash, 144 KB SRAM
SKY13373-460LF	1	0.519	RF Switch ICs .1-6.0GHz SP3T IL .45dB @ 2.5GHz
TPS629206DRLR	1	0.524	Switching Voltage Regulators 3-V to 17-V, 0.6-A, low-IQ, synchronous buck converte -40 to 150

This report is available at no cost from the National Laboratory of the Rockies (NLR) at www.nlr.gov/publications

Part Number	Qty	Unit Price $	Description
PTS810SJM250SMTRLFS	2	0.302	Tactile Switches SWITCH TACTILE
CY7C65211-24LTXIT	1	1.560	USB Interface IC USB-Serial Single-CH Bridge
629722000214	1	1.930	WR-COM USB 2.0 Type C Receptacle Horizontal SMT
693072010801	1	2.210	WR-CRD Micro SD Card Connector Hinge Type
GJM0335C1ER70WB01D	1	0.013	Multilayer Ceramic Capacitors MLCC - SMD/SMT 0.7 pF 25 VDC 0.05 pF 0201 C0G (NP0)
LQP03HQ1N0W02D	2	0.085	RF Inductors - SMD 1 NH .05%
GRM0335C1H1R0BA01J	3	0.005	CAPACITOR, CERAMIC C0G/NP0, 1pF, 50V, -0.1pF/+0.1pF, -55DEGC/+125DEGC, 0201, SMD
GRM155R61H105KE05D	6	0.013	Multilayer Ceramic Capacitors MLCC - SMD/SMT 1 uF 50 VDC 10% 0402 X5R
CRCW04022K20JNEDC	2	0.003	Thick Film Resistors - SMD 1/16watt 2.2Kohms 5% Commercial Use
GRM0335C1H2R2BA01J	1	0.010	CAPACITOR, CERAMIC C0G/NP0, 2.2pF, 50V, -0.1pF/+0.1pF, -55DEGC/+125DEGC, 0201, SMD
TMK105CBJ225KV-F	4	0.037	Multilayer Ceramic Capacitors MLCC - SMD/SMT 0402 25VDC 2.2uF 10% X5R
GRM0335C2A2R4WA01J	2	0.009	Multilayer Ceramic Capacitors MLCC - SMD/SMT 2.4 pF 100 VDC 0.05 pF 0201 C0G (NP0)
LQP03HQ2N5W02D	1	0.058	INDUCTOR, RF, CHIP, NON-MAGNETIC CORE, 2.5nH, -0.1nH/+0.1nH, 0.5A, -55DEGC/+125DEGC, 0201, SMD
GRM0335C1H3R0BA01J	3	0.004	CAPACITOR, CERAMIC C0G/NP0, 3pF, 50V, -0.1pF/+0.1pF, -55DEGC/+125DEGC, 0201, SMD
LQP03TN3N4B02D	2	0.016	RF Inductors - SMD 3.4 NH +-.1NH
GRM0335C1H3R6BA01J	1	0.007	CAPACITOR, CERAMIC C0G/NP0, 3.6pF, 50V, -0.1pF/+0.1pF, -55DEGC/+125DEGC, 0201, SMD
LQP03TN3N7B02D	2	0.003	RF Inductors - SMD 3.7 NH +-.1NH
LQP03HQ3N9B02D	3	0.019	INDUCTOR, RF, CHIP, NON-MAGNETIC CORE, 3.9nH, -0.1nH/+0.1nH, 0.5A, -55DEGC/+125DEGC, 0201, SMD
GJM0335C1E3R9WB01D	1	0.014	Multilayer Ceramic Capacitors MLCC - SMD/SMT 3.9 pF 25 VDC 0.05 pF 0201 C0G (NP0)
LQP03HQ4N7J02D	1	0.029	RF Inductors - SMD 4.7 NH 5%

This report is available at no cost from the National Laboratory of the Rockies (NLR) at www.nlr.gov/publications

Part Number	Qty	Unit Price $	Description
GRM0335C2A4R7WA01D	1	0.009	Multilayer Ceramic Capacitors MLCC - SMD/SMT 4.7 pF 100 VDC 0.05 pF 0201 C0G (NP0)
0402YD475MAT2A	2	0.029	Multilayer Ceramic Capacitors MLCC - SMD/SMT 16V 4.7uF X5R 0402 20%
CRCW04025K11FKED	3	0.001	Thick Film Resistors - SMD 1/16watt 5.11Kohms 1%
GRM0335C1H6R8WA01D	1	0.007	Multilayer Ceramic Capacitors MLCC - SMD/SMT 6.8 pF 50 VDC 0.05 pF 0201 C0G (NP0)
VLS201610HBX-6R8M-1	1	0.098	Fixed Inductors 6.8uH 0.98A 558mOhms Power Circuits
LQP03TN7N5HZ2D	1	0.012	INDUCTOR, RF, CHIP, NON-MAGNETIC CORE, 7.5nH, -3%/+3%, 0.3A, -55DEGC/+125DEGC, 0201, SMD
CRCW040210R0FKED	1	0.001	Dale Thick Film Resistors - SMD 1/16watt 10ohms 1%
CRCW040210K0FKEDC	4	0.002	Thick Film Resistors - SMD 1/16watt 10Kohms 1% Commercial Use
LQP03TN10NHZ2J	2	0.008	INDUCTOR, RF, CHIP, NON-MAGNETIC CORE, 10nH, -3%/+3%, 0.25A, -55DEGC/+125DEGC, 0201, SMD
GRM033R71E103KE14D	2	0.001	Multilayer Ceramic Capacitors MLCC - SMD/SMT 0.01 uF 25 VDC 10% 0201 X7R
GRM188R6YA106MA73D	3	0.032	Multilayer Ceramic Capacitors MLCC - SMD/SMT 10 uF 35 VDC 20% 0603 X5R
CRCW040211K5FKED	1	0.001	Thick Film Resistors - SMD 1/16watt 11.5Kohms 1% Commercial Use
LQP03TN12NHZ2D	2	0.004	RF Inductors - SMD 12 NH 3%
02013A120JAT2A	4	0.024	Multilayer Ceramic Capacitors MLCC - SMD/SMT 50V 12pF C0G 0402 5%
LQP03TN20NH02D	1	0.014	INDUCTOR, RF, CHIP, NON-MAGNETIC CORE, 20nH, -3%/+3%, 0.15A, -55DEGC/+125DEGC, 0201, SMD
LQP03TN22NHZ2D	1	0.019	INDUCTOR, RF, CHIP, NON-MAGNETIC CORE, 22nH, -3%/+3%, 0.15A, -55DEGC/+125DEGC, 0201, SMD
GRM188R60J226MEA0D	3	0.014	Multilayer Ceramic Capacitors MLCC - SMD/SMT 0603 22uF 6.3volts *Derate Voltage/Temp
LQP03TN27NH02D	1	0.012	RF Inductors - SMD 27 NH 5%
ECS-.327-9-16-TR	1	0.412	Crystals 32.768kHz 9pF -40C +85C

This report is available at no cost from the National Laboratory of the Rockies (NLR) at www.nlr.gov/publications

Part Number	Qty	Unit Price $	Description
CRCW040234K0FKED	2	0.001	Thick Film Resistors - SMD 1/16watt 34Kohms 1% Commercial Use
GRM21BR61A476ME15L	1	0.106	Multilayer Ceramic Capacitors MLCC - SMD/SMT 47UF 10V 20% 0805
TG2016SMN 48.0000M-MCGNNM0	1	0.503	TCXO Oscillators TG2016SMN 48.0000M-MCGNNM0: TCXO 2.8V 3.3V 0.5PPM -40 85C NON O/E 1K TR
GRT155R71H104KE01D	26	0.002	Multilayer Ceramic Capacitors MLCC - SMD/SMT 0.1 uF 50 VDC 10% 0402 X7R AEC-Q200
GRM0335C1H101GA01D	9	0.003	CAPACITOR, CERAMIC C0G/NP0, 100pF, 50V, -2%/+2%, -55DEGC/+125DEGC, 0201, SMD
CRCW0402154KFKED	2	0.002	Thick Film Resistors - SMD 1/16watt 154Kohms 1% Commercial Use
GRM155R61J334ME01D	1	0.012	Multilayer Ceramic Capacitors MLCC - SMD/SMT 0402 X5R 0.33 F 20 63VDC
CRCW0402383KFKED	1	0.002	Thick Film Resistors - SMD 1/16watt 383Kohms 1%
CRCW0402470RFKED	5	0.001	Thick Film Resistors - SMD 1/16watt 470ohms 1%
HCUCC PCB REV 1	1	0.600	PCB Manufacturing
HCUCC Component ASSY and Testing	1	1.000	Part of the manufacturing process
		26.560	TOTAL

Note the above part numbers are searchable online if more detail is desired.

This report is available at no cost from the National Laboratory of the Rockies (NLR) at www.nlr.gov/publications